AFWAL-TM-87-160-FIMG

ON PREDICTING HYPERSONIC BOUNDARY LAYER TRANSITION

KENNETH F. STETSON
HIGH SPEED AERO PERFORMANCE BRANCH
AERONECHANICS DIVISION

MARCH 1987

FLIGHT DYNAMICS LABORATORY
AIR FORCE WRIGHT AERONAUTICAL LABORATORIES
WRIGHT-PATTERSON AIR FORCE BASE, OHIO 45433

FOREWORD

The purpose of this document is to provide information that may be useful for predicting hypersonic boundary layer transition. This work was conducted by the High Speed Aero Preformance Branch (AFWAL/FIMG), Aeromechanics Division, Flight Dynamics Laboratory, Air Force Wright Aeronautical Laboratories, Wright-Patterson Air Force Base, Ohio.

This technical memorandum has been reviewed and approved.

Valentine Dahlem

VALENTINE DAHLEM
Chief, High Speed Aero Performance Branch
Aeromechanics Division

TABLE OF CONTENTS

PAGE

INTRODUCTION.. 1

PART I: BACKGROUND INFORMATION...................................... 2

1. ALL TRANSITION PREDICTION METHODS ARE EMPIRICAL.................. 2

2. MANY PARAMETERS AFFECT TRANSITION................................ 2

a. MACH NUMBER.. 5

b. NOSETIP BLUNTNESS.. 6

c. ANGLE OF ATTACK.. 10

d. UNIT REYNOLDS NUMBER... 11

e. ENVIRONMENT.. 13

f. WALL TEMPERATURE... 16

g. SURFACE ROUGHNESS.. 18

h. PRESSURE GRADIENT.. 19

i. MASS TRANSFER.. 20

j. REAL GASES/NON-EQUILIBRIUM....................................... 20

k. BODY CURVATURE... 21

l. VIBRATION.. 21

3. ONE MUST HAVE AN EXPERIMENTAL DATA BASE TO ESTABLISH THE EMPIRICAL RELATIONSHIPS.. 22

4. ALL TRANSITION PREDICTION METHODS HAVE SERIOUS DEFICIENCIES..... 24

5. WIND TUNNEL TRANSITION REYNOLDS NUMBERS ARE GENERALLY LOWER THAN CORRESPONDING FLIGHT TRANSITION REYNOLDS NUMBERS............... 26

6. SOMETIMES UNEXPECTED PHENOMENA CAN GREATLY REDUCE THE EXPECTED TRANSITION REYNOLDS NUMBER..................................... 27

7. THERE ARE UNIQUE FEATURES OF HYPERSONIC TRANSITION............ 29

8. THE LENGTH OF THE TRANSITION REGION VARIES.................... 32

9. CALCULATIONS OF BOUNDARY LAYER PROPERTIES ARE IMPORTANT........ 34

PART II: COMMENTS ON SEVERAL TRANSITION PREDICTION METHODS............ 35

1. $Re_{\Theta T}/M_e$ = CONSTANT.. 35

2. $Re_{\Theta T}$ vs X/R_N.. 36

3. e^N.. 39

PART III: SOME THOUGHTS ON HOW TO PREDICT HYPERSONIC TRANSITION IN 1987. 41

1. NOSETIP.. 41

2. EARLY FRUSTUM.. 42

3. FRUSTUM.. 43

a. ZERO PRESSURE GRADIENT.. 43

b. WITH PRESSURE GRADIENT.. 44

REFERENCES.. 46

APPENDIX.. 50

FIGURES.. 58

NOMENCLATURE

A	Disturbance amplitude (arbitrary units)
k	Roughness height
kHZ	Kilohertz
K	Entropy layer swallowing constant
M	Mach number
N	Ln(A/Ao)
p	Pressure (psia)
R	Radius (inches)
Re	Reynolds number
Re_{XT}, $Re_{\delta T}$	Transition Reynolds number based upon conditions at the edge of the boundary layer and surface distance from the sharp tip or stagnation point to the location of transition
Re_{θ}	Reynolds number based upon conditions at the edge of the boundary layer and the laminar boundary layer momentum thickness
T	Temperature (R)
U	Velocity
u'	Velocity fluctuations
X, S	Surface distances (inches or feet)
X_{sw}	Entropy layer swallowing distance (see Fig. 4) (inches or feet)
X_T	Surface distance from the sharp tip or stagnation point to the onset of transition (inches or feet)
α	Angle of attack (deg)
δ	Boundary layer thickness (inches)
θ	Laminar boundary layer momentum thickness (inches)

θ_c	Cone half angle (deg)
λ	Wavelength of disturbance
ϕ	Cone meridian angle (deg.)

Subscripts

AD	Adiabatic
B	Beginning or blunt
e, δ	Edge of boundary layer
E	End
N	Nose
O	Reservoir or initial
S	Sharp
ST	Model stagnation point
T	Transition
W	Wall
∞	Freestream

INTRODUCTION

Boundary layer transition is a problem which has plagued several generations of aerodynamicists. Researchers have been frustrated by many unsolved transition phenomena, by the fact that transition sometimes bypasses the known linear processes, and by the difficulties of sorting out the many interrelated and complicated effects and isolating the various parameters for investigation. Transition predictors are confronted with many transition prediction methods, most of which have some merit, but all with serious limitations which are often not adequately known to the user.

Many papers have been written over the years on various aspects of boundary layer transition. Very few papers have specifically addressed the general problem of predicting boundary layer transition from the point of view of providing background information for the transition predictors. A report by Morkovin[1], although written nearly 20 years ago, provides much valuable information which continues to be pertinent to hypersonic transition. References 2-4 are some examples of other papers which should be read for additional background information. Also, a recent paper by Reshotko[5] makes an important contribution in this area. Reshotko reviews the present status of our knowledge of transition, and, although hypersonic transition is not specifically addressed, many of the topics discussed apply to the entire velocity spectrum. The renewed interest in hypersonic flight is believed to warrant further documentation of the problem of predicting hypersonic transition. It is not the intent of this paper to recommend a specific correlation technique for predicting hypersonic transition, primarily because there is no good, general hypersonic transition prediction method to recommend. Available correlation techniques emphasize special aspects of the problem and usually have severe limitations when they are applied to configurations or flow conditions outside the range of the data which were used to generate the empirical relationship of the correlation. Often a transition predictor adopts a particular method and then uses it for all situations, as though it had a general application. What is desired here is to provide some background information, along with some comments about several prediction methods, to help the transition predictor become more aware of the limitations of the prediction methods and to understand under what circumstances they should be used. No attempt has been made to provide an extensive review of the literature or a complete bibliography. The various topics are discussed briefly, with comments on those aspects of the problems that a failing memory could retrieve. It is realized that important points may have been omitted and, if time were available for a more complete review of the literature, many topics would probably be rewritten. Many of the comments represent personal opinions, or opinions of associates, and should not, in any way, be considered the final answers. Many aspects of transition are controversial and differences of opinion are common. Debate of these complicated issues are considered necessary and worthwhile. It is hoped that these remarks can be used as a starting point for much continued discussion and, in this regard, reader comments are solicited. Consideration will be given to a revised paper at a future date.

PART I: BACKGROUND INFORMATION

There are several profound facts that one should consider in predicting hypersonic boundary layer transition:

1. ALL TRANSITION PREDICTION METHODS ARE EMPIRICAL

Stability theory can show that the boundary layer will be unstable above certain Reynolds numbers and provide the growth rates for the unstable disturbances, but it can not predict turbulence. It has never been proven mathematically that turbulent flow is the proper state at high Reynolds numbers. Turbulence is an experimentally observed fact. The relationship between boundary layer stability and transition is not well understood. There is no transition theory.

2. MANY PARAMETERS AFFECT TRANSITION

The transition of a laminar boundary layer to turbulence is a complex phenomena which is influenced by many contributing factors. An attempt to express the functional relationship would look something like the following:

$$(Re)_{\text{transition}} = f\left(M, \theta, T_w, \dot{m}, \alpha, k, E, \frac{\partial p}{\partial X}, R_N, \frac{Re_\infty}{FT}, \frac{X}{R_N}, V, C, \frac{\partial \omega}{\partial z}, T_0, d^*, \tau, Z\right)$$

where

M = Mach number

θ = Cone angle or configuration characteristic

T_w = Wall temperature

$\dot{m}$ = Mass addition or removal

α = Angle of attack

k = Roughness

E = Environment

$\frac{\partial p}{\partial x}$ = Pressure gradient

Rn = Nosetip radius

Re_∞/FT = Unit Reynolds number

X/R_N = Location in the entropy layer

V = Vibration

C = Body curvature

$\frac{\partial w}{\partial z}$ = Cross flow

To = Stagnation temperature

d* = Characteristic dimension

τ = Chemical reaction time

Z = Compressibility factor (or some accounting for real gas effects)

Of course, not all of these parameters are important in a given flow situation. Also, those parameters which do effect transition have varying strengths, and sometimes one parameter can have a dominating effect (e.g., nosetip bluntness or roughness). It is not possible to include enough parameters into an empirical relationship to have a transition correlation general enough to handle a variety of situations. This is the basic problem which transition predictors face. Usually an attempt is made to include the dominant parameters and the others are neglected. Therefore, most transition correlations relate to specific configurations and flow situations. If a correlation of the form, Re vs X/R_n, is developed, all of the other effects become hidden in the functional relationship. When applying this correlation to a new situation, it is assumed (perhaps unknowingly) that all of the hidden effects are unchanged. The problem is that rarely do the hidden effects remain unchanged and rarely can we predict how much they will change. The result is that transition prediction methods have an unknown uncertainty when applied to new situations. It is important that we try to better understand the uncertainty of transition predictions.

Following are brief comments regarding the major parameters influencing boundary layer transition:

Effect of Mach Number: For many years wind tunnel transition data had been put in the format of transition Reynolds number vs Mach number. There were significant variations in the magnitude of transition Reynolds, yet the trends were generally the same. Between $M \cong 1$ and 2.5-3, transition Reynolds number decreased with increasing Mach number and a minimum occurred at $M = 3$-4. Further increases in Mach number consistently increased the transition Reynolds number. Fig I (from Ref. 6) illustrates this trend. The disturbances in the freestream of a wind tunnel, generated by the turbulent boundary layer on the nozzle wall, clearly have a large effect on transition on models in wind tunnels. The decrease in transition Reynolds number with Mach number in the supersonic range is most likely the result of the disturbances in the freestream of the wind tunnels. Flight experiments on a 5-deg half angle cone supported this contention by demonstrating that transition Reynolds number increased with Mach number up to $M = 2$ (the maximum Mach number of the experiment). Fig. 2 shows some of the flight data and compares flight transition data with wind tunnel transition data.

All data were obtained with the same model and same instrumentation (Fig. 2 is from Ref. 7). Wind tunnel results at hypersonic Mach numbers have consistently showed a large increase in transition Reynolds number with increasing Mach number. Unfortunately it has not been possible to separate out the wind tunnel effects and the Mach number effects. Most experimenters have speculated that the Mach number effect in the hypersonic regime is one of increasing transition Reynolds number with increasing Mach number. This conclusion is further supported by theory. The stability theory of Mack[4] has shown that, at hypersonic Mach numbers, the maximum amplification rates decrease as the Mach number increases. A decrease in the maximum amplification rate would be expected to result in larger transition Reynolds numbers. The Mach number effect may not be as pronounced in flight transition data as in wind tunnel transition data since in a wind tunnel the environment varies with the Mach number. Fig. 3 (from Ref. 8) includes additional data to illustrate Mach number effects on transition. Both wind tunnel and flight results are shown and an attempt has been made to separate out unit Reynolds number effects.

Available data suggests that high transition Reynolds numbers are to be expected when the local Mach number is like 10 or above. There is considerable uncertainty as to the magnitude or the functional relationship between transition Reynolds number and Mach number. The correlation, Re_θ/Me = constant, requires a judgement as to this functional relationship. This topic will be discussed in more detail under Part II.

Effect of Nosetip Bluntness: Wind tunnel experiments[9,10] at M = 6 and M ≅ 9, along with shock tunnel experiments[11], have demonstrated that nosetip bluntness has a large effect on transition on the frustum of a slender cone. Small nosetip bluntness increases the transition Reynolds number and large nosetip bluntness decreases the transition Reynolds number relative to the sharp cone. Also, the local Reynolds number is reduced as a result of nosetip bluntness and this can have a large effect on the location of transition. The nosetip of a sphere-cone configuration in hypersonic flow generates high entropy fluid (usually referred to as the entropy layer) which is subsequently entrained in the boundary layer as the boundary layer grows on the frustrum. This is illustrated in Fig. 4 (from Ref. 9). The extent of the frustrum boundary layer influenced by the high entropy fluid and the boundary layer edge conditions at a given frustum station depend upon both geometric and flow parameters. For a slender cone in hypersonic flow, and particularly with the thinner boundary layers associated with a cold wall condition, the entropy layer extends for many nose radii downstream (e.g., several hundred). In Fig. 5, boundary layer calculations illustrate the large effect of a 0.04 in. nosetip radius (from Ref. 9).

In order to account for nosetip bluntness effects upon transition, the entropy layer effect should be considered. A simple and easy method for estimating the extent of the entropy layer and variations of boundary layer edge conditions can be made by assuming sphere-cone configurations and similarity of flows. For example, the method of Rotta[12], permits such estimates without the use of local flow field calculations. Note that Rotta's method only applies to the case of highly cooled walls. Fig. 6 (from Ref. 9) provides a method to estimate entropy layer swallowing distances for highly cooled sphere-cones. Of course, if one has boundary layer calculations available for a case in question, the entropy layer effects are included in those results. A number of comparisons of entropy layer swallowing distances estimated by the method of Rotta were found to correspond to locations where boundary layer code results indicated the local Mach number was 96 to 98 percent of the sharp cone value. This is considered to be excellent agreement. The two major effects associated with the entropy layer are changes in the transition Reynolds number and reductions in the local Reynolds number. The reduction of the local Reynolds number is an extremely important piece of information in the interpretation of nosetip bluntness effects on frustum transition; however, this is not the major issue since this information is readily obtainable, with uncertainties being related only to the accuracy and limitations of the flow field program being utilized. The major problem area is associated with understanding how nosetip bluntness affects the transition Reynolds number. Limitations in the Reynolds number capability of wind tunnels has limited wind tunnel results to Mach numbers less than 10. These results are useful to illustrate trends; however, the effects of higher Mach numbers and the magnitude of transition Reynolds numbers expected in free flight are not well known. Fig. 7 (from Ref. 9) contains the results from a large amount of nosetip bluntness data obtained in a Mach 6 wind tunnel. The movement of transition location is shown, along with changes in transition Reynolds number and the Reynolds number reduction which contributed to the changes in transition location. Note that when the entropy layer was nearly swallowed at the transition location (X_T/X_{SW} close to 1), the transition Reynolds numbers were significantly larger than sharp cone transition Reynolds numbers and the Reynolds number reduction was small. The change in transition location in this region was primarily a function of the change in transition Reynolds number. The maximum change in transition location occurred in regions of the entropy layer where the transition Reynolds numbers were less than the sharp cone values and the Reynolds number reduction was the major effect. For maximum transition displacement, the local Reynolds number was reduced by a factor of 7.3 and the transition Reynolds number was 58% of the sharp cone value, with the displacement being represented by the product of the two effects, or 4.2 times the sharp cone transition location.

The Reentry F flight experiment[13,14] is probably the best source of data for the effect of nosetip bluntness on slender cone transition in hypersonic free flight. The lack of information regarding the nosetip changes during reentry as a result of ablation, along with small angles of attack, produce some uncertainties in the interpretation of the results.

There is another nosetip consideration that should be included - the very low transition Reynolds numbers associated with transition on the nosetip and the region of the frustum just downstream of the nosetip. Nosetip transition Reynolds numbers can be as much as two orders of magnitude less than cone frustum transition Reynolds numbers. This situation requires that a separate transition criteria be applied to this portion of a configuration. The potential of transition first occurring in this region, and producing a turbulent boundary layer over the entire portion of the configuration influenced by the tip, must be considered. It is well documented that blunt nosetips have low transition Reynolds numbers, even at hypersonic freestream Mach numbers (e.g., Refs. 15-17). Boundary layer transition has been related to the local boundary layer properties at the sonic point and the surface roughness. The low transition Reynolds numbers associated with the region of the frustum just downstream of the nosetip has only recently been identified[9] and the transition criteria for this region is not as well understood as that of the nosetip. It appears that transition in this region is dominated by the nosetip and may be related to nosetip conditions, analogous to nosetip transition criteria. Fig. 8 (from Ref. 9) provides an example of transition criteria for transition on the nosetip and also those conditions which produced early frustum transition for Mach 5.9 wind tunnel experiments. Nosetip transition (often referred to as the "Blunt Body Paradox") is discussed further under transition bypasses (Part I, Section 6) and under Part III.

Effect of Angle of Attack: Intuition derived from boundary layer transition results at zero angle of attack is not very helpful in predicting the transition trends on a sharp cone at angle of attack. The effect of angle of attack is to increase the local Reynolds number and decrease the local Mach number on the windward ray. One might logically assume that transition would then move forward on the windward ray with increases in angle of attack. On the leeward ray the local Reynolds number decreases and the local Mach number increases. Based upon results obtained at zero angle of attack, it might be expected that transition would move rearward on the leeward ray with increases in angle of attack. In reality, just the opposite of these trends occur. Transition experiments with a sharp cone have consistently found a rearward movement of transition on the windward ray and a forward movement on the leeward ray (see, for example, Ref. 18). Transition location was found to be sensitive to small changes in angle of attack for both sharp and blunt-tipped configurations. For configurations with nosetip bluntness one has to consider the combined effects of nosetip bluntness and angle of attack. The angle of attack trends appear to be predictable; however, the magnitude of the resulting transition Reynolds numbers are not. Fig. 9 (from Ref. 18) illustrates the transition movement on the windward and leeward rays of sharp and blunt 8-deg. half angle cones at $M_\infty = 5.9$. The transition distance (X_T) is normalized by the transition distance on the sharp cone at $\alpha = 0$ deg. [$(X_{TS})_{\alpha = 0}$ varies with unit Reynolds number]. Fig. 10 (from Ref. 18) is a sample of the transition patterns obtained for a sharp cone. ϕ = 0 deg. is the windward meridian and ϕ = 180 deg. is the leeward meridian. The shaded area represents the transition region, with curve B indicating the beginning of transition and curve E the end of transition. The beginning and end of transition at α = 0 deg. is shown for reference. Fig. 11 (from Ref. 18) presents a summary of the sharp cone angle of attack results, in a nondimensionalized format. Figures 12 and 13 (from Ref. 18) present similar results for a cone with 10% nosetip bluntness (R_n = 0.2 in).

Effect of Unit Reynolds Number: For some time there has been evidence that transition Reynolds number was influenced by the unit Reynolds number. Numerous wind tunnel experiments have documented the result that increasing unit Reynolds number increases the transition Reynolds number. A suitable explanation and an accounting of the phenomena involved is still not complete. Because the examples of this effect were almost exclusively from wind tunnel experiments and because of the possibility that wind tunnel freestream disturbance were responsible, there has been uncertainty as to whether the so-called unit Reynolds number effect exists in free flight. Potter[19,20] performed extensive ballistic range experiments to investigate unit Reynolds number effects in ballistic ranges. Potter's conclusions were that a unit Reynolds number effect existed in the free flight range environment. In fact, the increases of transition Reynolds number with increases in unit Reynolds number were even larger in the ballistic range than in wind tunnels. He found that none of the range-peculiar conditions could offer an explanation for this effect. Fig. 14 (from Refs. 19 and 20) is a sample of Potter's results. Additional discussions of unit Reynolds number effects on transition have been made by Reshotko[21] and Stetson[22]. Unit Reynolds number effects have a very important coupling with environmental effects. For a low disturbance environment, the environmental disturbances provide the stimulus for exciting boundary layer disturbance growth and are responsible for the initial boundary layer disturbance amplitudes. If, by some mechanism, the initial amplitude of the most unstable boundary layer disturbances could be increased or decreased, the transition Reynolds number would correspondingly be increased or decreased (this will be discussed under the next topic, environmental effects). The unit Reynolds number, in effect, provides a possible mechanism. The frequencies of the most unstable boundary layer disturbances are directly related to the unit Reynolds number (this topic is discussed under Part I, Section 7). Thus, increasing unit Reynolds number increases the frequency of the most unstable boundary layer disturbances, which means that the most important environmental disturbances are of higher frequency. The higher frequency environmental disturbances will, very likely, have a smaller amplitude and, in some situations, a suitable environmental stimulus may be lacking for some frequencies. Also, increasing unit Reynolds number will, very likely, increase the minimum Reynolds number at which boundary layer disturbances first start to grow, which would be expected to increase the transition Reynolds number. Intuitively, it would be expected that unit Reynolds number, through its control of the frequency of the most unstable boundary layer disturbances, would influence transition.

The conclusion is that unit Reynolds number effects on transition are expected in free flight. However, without knowledge of the disturbance environment through which the vehicle is flying and a better understanding of the physical mechanisms which cause transition, it is not possible to predict the magnitude of these effects.

Effect of the Environment: The environment provides an extremely important initial condition for any boundary layer transition problem. This critical element of the problem is often overlooked by people making transition predictions. The environment provides the mechanism by which boundary layer disturbance growth is generally initiated and establishes the initial disturbance amplitude at the onset of disturbance growth. If we change the environment we will most likely change the transition Reynolds number. When one or several sets of data are used to make a transition prediction in a new situation, a similarity is implied for not only the geometric and flow parameters, but also the environment. It is assumed that the case in question has the same environment as the data base. Environmental differences provide a reasonable explanation for the difference in transition Reynolds numbers obtained in wind tunnels and those obtained in free flight. In supersonic and hypersonic wind tunnels the strong acoustical disturbances in the freestream which are generated by the turbulent boundary layer on the wall of the nozzle generally produce transition Reynolds numbers lower than found in free flight. Differences in wind tunnel environments can result in significant differences among wind tunnel transition Reynolds numbers, thus presenting problems in correlating only wind tunnel transition data. The data of Schubauer and Skramstad[23] and Wells[24] provide an interesting example. The classical experiments of Schubauer and Skramstad were carried out on a sharp, flat plate in a low turbulence, low speed wind tunnel (these experiments provided the first demonstration of the existence of instability waves in a boundary layer, their connection with transition, and the quantitative description of their behavior by the theory of Tollmien and Schlichting). Turbulence levels in the freestream could be controlled by varying the number of damping screens.

Transition Reynolds numbers were found to be directly related to the freestream turbulence level, with transition Reynolds number increasing as the turbulence level decreased. At low tunnel turbulence levels, the transition Reynolds number obtained a maximum value of 2.8×10^6 and remained at this level with still further reductions in turbulence levels. Wells repeated this experiment in a different wind tunnel. In the Schubauer and Skramstad experiment, control over the damping screens provided control over the velocity fluctuations in the freestream of their wind tunnel but the screens had little effect on the acoustical disturbances which were present. In the Wells experiment, the tunnel was designed so as to minimize the acoustical disturbances as well as to provide control over the velocity fluctuations. Wells found the same trends as obtained by Schubauer and Skramstad, but his maximum transition Reynolds number was approximately 5×10^6. Both experiments were dealing with the same boundary layer phenomena. What was different was the environment. Fig. 15 (from Ref. 24) contains these results. Wells indicated that most of the energy in his experiment occurred at frequencies below 150 cps with acoustic content less than 10% of the total energy. The tests of Schubauer and Skramstad involved significant energy levels out to 400 cps, and, in addition, the spectrum exhibited large acoustic energy peaks at 60 and 95 cps which accounted for approximately 90% of the total disturbance energy that was measured for intensities less than about 0.05%. Spangler and Wells[25] continued the study by systematically investigating the effects of acoustic noise fields of discrete frequencies. Large effects were found when the acoustic frequencies (or a strong harmonic) fell in the range where Tollmien-Schlichting waves were unstable. It is significant to note that transition prediction methods; for example, the e^N method, can not account for these large differences in transition Reynolds number unless the differences in the freestream environment are somehow taken into account.

Environmental disturbances are predominantly of low frequency and the most unstable hypersonic boundary layer disturbances are of relatively high frequency. Thus an important consideration for hypersonic boundary layer transition is whether or not the disturbance environment will provide a suitable stimulus to excite the most unstable boundary layer disturbances. Normally one would expect the most unstable disturbances to have the most rapid growth and be the first disturbances to obtain the critical amplitude which produced nonlinear effects and the eventual breakdown of the laminar flow. If transition must wait for disturbances with a smaller growth rate to obtain the critical amplitude, then a delay in transition would be expected. There are many hypersonic flow situations, both in ground test facilities and in free flight, where the potentially most unstable boundary layer disturbances may not be excited. Thus, some transition delay, due to a lack of environmental stimulus of the potentially most unstable disturbances, may be a common hypersonic occurrence. Stetson[26] has pointed out that for a sharp, 7-deg half angle cone in a Mach number 8 wind tunnel at a freestream unit Reynolds number of 20 million, the most unstable boundary layer disturbances would have frequencies greater than a megahertz. Available instrumentation can not measure disturbances in this frequency range; however, it seems unlikely that there would be much freestream disturbance energy at such high frequencies to stimulate boundary layer disturbance growth. Transition under this situation would be expected to be the result of disturbances which were not the theoretically most unstable. This should provide larger transition Reynolds numbers. The Reentry F flight experiment[13] reported transition

Reynolds numbers as high as 60 million. An estimation of the frequency of the most unstable boundary layer disturbances indicated they were greater than 500 kHZ. There is a possibility that these high transition Reynolds numbers were obtained because the theoretically most unstable disturbances were not present.

Another important aspect of the disturbance environment is the receptivity (Morkovin[1]) of the boundary layer to these disturbances. The characteristics of the disturbance environment which eventually interacts with the boundary layer and the response of the boundary layer to these disturbances has long been recognized as an important problem; however, an understanding of this problem has been slow to develop. Reshotko has discussed the receptivity problem in several papers [3,5,27].

The sobering environmental conclusion is that even if we could perform a miracle and obtain an analytical method to calculate exactly the stability characteristics of the boundary layer and the breakdown to turbulence, we would still have problems predicting transition because we would still have to somehow prescribe the external disturbances. The freestream disturbances are a very important initial condition of any boundary layer transition problem and, unfortunately, they are generally not well known. The uncertainty of the disturbance environment in free flight puts an additional uncertainty into any transition prediction.

<u>Effect of Wall Temperature</u>: The temperature of the surface of a vehicle or model can have a large effect on boundary layer transition. One of the results from the compressible stability theory of Lees[28] was the prediction that cooling the wall would stabilize the boundary layer. Calculations were subsequently made which indicated that, with sufficient cooling, the boundary

layer could be made completely stable at any Reynolds number (e.g.,Van Driest[29]). A number of experiments followed to verify the prediction of the stabilizing effect of wall cooling. The results demonstrated one more time the complicated, interrelated involvement of transition parameters. The trend of increasing transition Reynolds numbers with increasing wall cooling was confused by a transition reversal. That is, situations occurred in which the stabilizing trend of wall cooling was reversed and further cooling resulted in a reduction of transition Reynolds number. In very highly cooled cases, there was evidence of a re-reversal, a return to a stabilizing trend. Fig. 16 (from Ref. 11) illustrates some of these results. There were attempts to explain transition reversal on the basis of a surface roughness effect; however, much of the data did not seem to support the roughness agreement. Transition reversal, as a result of wall cooling, has remained a controversial subject.

The wall cooling situation is even further confused in hypersonic flows. It is not recognized by many that the theoretical arguments of the stabilizing effect of wall cooling did not consider the high frequency instabilities (the Mack modes) of hypersonic flow. Mack[4] has pointed out that second mode disturbances are the major instabilities in hypersonic flow and these disturbances are not stabilized by surface cooling but, in fact, are destabilized. Hypersonic wind tunnel transition results have provided conflicting results in this area and have not clarified the situation. This could be due to the fact that the role of second mode disturbances in hypersonic wind tunnel transition experiments is generally unknown. As pointed out in the previous section, the most unstable second mode disturbances may not be excited in many hypersonic flow situations, thus the destabilizing effect of wall cooling would be minimized or eliminated. Hot-wire experiments of

Stetson et al[22] have demonstrated a hypersonic case where second mode disturbances were the major disturbances and wall cooling produced significantly lower transition Reynolds numbers. Demetriades'[33] hot-wire experiments at Mach 8 demonstrated that second mode disturbances amplified at a faster rate on a cold wall than on a model with an equilibrium temperature wall. The lower transition Reynolds numbers he obtained for the cold wall case could be approximately accounted for by the corresponding increases in the disturbance amplification rates.

Surface temperature is seen to have a potentially large effect on hypersonic boundary layer transition, with wall cooling expected to be stabilizing for first mode disturbances and destabilizing for second mode disturbances. The problem is that unless the identify of the major disturbances is known (or predictable) one does not even know if the proper trend is increasing or decreasing transition Reynolds number.

<u>Effect of Surface Roughness</u>: The physical mechanisms by which roughness effects transition are not well understood. Usually the only parameter measured is the movement of transition location and the details of what is causing the movement are unknown. Small roughness is not believed to generate hypersonic boundary layer disturbances. It can effect transition by changing the mean flow characteristics of the boundary layer in such a manner as to increase the growth rate of disturbances already present in the boundary layer. Experiments have shown there is a minimum size of roughness elements which will influence transition. Below this minimum the surface is considered to be aerodynamically smooth. If roughness elements are large enough to generate locally separated flow about the roughness elements, they can produce small regions of turbulence which can become a mechanism for exciting new

boundary layer disturbance growth. In this case, roughness not only increases the growth rate of those disturbances already present, but introduces new disturbances. It is speculated that such a mechanism may be responsible for exciting boundary layer disturbance growth in free flight in a frequency range where the freestream environment had not provided the stimulus. Large roughness greatly distorts the boundary layer and further complicates an understanding of the phenomena. The relative size of roughness elements is usually determined by comparing it to the boundary layer thickness. Any effect which influences boundary layer thickness can affect the influence of roughness. Therefore, body location, unit Reynolds number, wall temperature, Mach number, and mass addition or removal can all influence the effect of roughness. Wind tunnel experiments have shown there is a strong effect of Mach number on roughness effects. The roughness size required to trip the boundary layer increases rapidly with increasing Mach number and even at low hypersonic Mach numbers the roughness heights required are of the same order as the boundary layer thickness (e.g., see Ref. 34). Part of the problem in trying to understand roughness effects is associated with the many roughness parameters involved. In addition to roughness height, configuration and spacing are important. Also important are whether they are two-dimensional or three-dimensional elements, individual elements or distributed (e.g., sand grain) type.

Effect of Pressure Gradient: The general effects of pressure gradients are well known for situations where transition results from first mode instabilities. Both theory and experiment have shown that favorable pressure gradients stabilize the boundary layer and adverse pressure gradients destabilize the boundary layer. In many cases pressure gradient effects are simultaneously combined with other effects so the resultant effect is not always as expected. Stetson[9] has illustrated a hypersonic flow situation (the local Mach number was supersonic) on a sphere-cone where the transition Reynolds number decreased as the favorable pressure gradient increased (moving closer to the nosetip). Apparently the destabilizing effect of the nosetip was more powerful than the stabilizing effect of the pressure gradient. Also, the same paper reports that the adverse pressure gradient on the cone frustum did not have a significant effect on transition.

There is not sufficient information available to make a prediction of the effect of a specific pressure gradient on hypersonic boundary layer transition. About the best one can do at this time is make an estimate.

Effect of Mass Transfer: As with pressure gradients, mass transfer effects can be described only in a general way. Experiments have shown that suction stabilizes the boundary layer. It produces a "fuller" velocity profile, just as a favorable pressure gradient, and a more stable boundary layer. Blowing destabilizes the boundary layer, analogous to the adverse pressure gradient. Details of the effects of mass flow weights, gas composition, and mass transfer methods are too sketchy to be of much assistance in predicting the effects of mass transfer on hypersonic boundary layer transition in a specific situation. Mass transfer effects must also be considered in combination with other effects; for example, its effect on roughness and surface cooling.

Wind tunnel experiments by Martellucci[35] confirmed that mass transfer had a destabilizing effect upon the boundary layer. He noted that the effects of mass transfer were much like surface roughness. When the mass was injected at a subcritical value, no influence on transition was noted; however, at a discrete value of blowing (termed the critical value) transition was affected and moved rapidly forward.

Effect of Real Gases/Non-Equilibrium: This is an area which has not really been addressed. Using linear stability theory as a guide, any effect which changes the boundary layer profiles will influence boundary layer stability. Therefore, real gas and non-equilibrium effects would be expected to influence transition. Ground test facilities will not be of much help due to their limitations, so flight test results must be relied upon for the answers. Some real gas, equilibrium flow conditions must have existed for the reentry vehicles in the Mach 20 regime. The non-equilibrium effects will be a new phenomenon associated with high altitude flight and will be an unknown factor that should be considered in the uncertainty of a transition prediction at high altitudes.

Effect of Body Curvature: Body curvature has other effects besides changing the inviscid pressure distribution. Concave surfaces are known to generate Görtler instabilities. Most information about Görtler instabilities have been obtained at low velocity, where they are believed to have a dominant effect on boundary layer transition. Morkovin has commented that the presence of Görtler instability is often suspected, but seldom documented; mostly because of the difficulty of measuring steady streamwise vorticity. For convex surfaces consideration should be given to the effects of angular momentum on boundary layer transition.

Body curvature effects on hypersonic boundary layer transition are pretty much an open question.

Effect of Vibration: Vehicle or model vibration is not normally considered to be a major parameter influencing boundary layer transition. However, for a vehicle which has an operating engine, vibration effects should not be ignored. Intuitively one would expect structural vibrations to be at such a low frequency relative to the most unstable boundary layer frequencies, that they would be of little consequence.

3. ONE MUST HAVE AN EXPERIMENTAL DATA BASE TO ESTABLISH THE EMPIRICAL RELATIONSHIPS

Since all transition prediction methods are empirical, an experimental data base is a necessary requirement in establishing a transition prediction method. The availability of a data base, per se, is not a problem since much experimental transition data have been obtained over the past years. The problem is that one seldom has the right data available. Transition experiments document the location of the breakdown of laminar flow and how some flow or geometric parameter causes that location to move. The specific details of the phenomena involved are usually lacking and the interpretation of the transition data becomes difficult and speculative. If an attempt is made to utilize a variety of results in a single transition plot, the large variations of results will generally make it impossible to establish a meaningful empirical relationship. Fig. 17 (from Ref. 36) illustrates the problem. It becomes essential to be selective in the data used and to include only those data which most nearly correspond to the problem in question. The decision of what data to use in the establishment of an empirical relationship and the transition criteria is always a difficult choice since it can have a large effect on the resulting transition predictions. Such a procedure then limits the generality of the prediction method. The trend seems to be that improvements to the prediction method are made only at the expense of greater limitations on the application of the method. It is clear that one should always know what data were used to establish the transition prediction method being considered.

When it becomes necessary to predict transition on a new configuration or at new flow conditions empirical prediction methods have problems. The data base can only be used as a guide and any transition prediction for such a situation will have a large uncertainty associated with it.

4. ALL TRANSITION PREDICTIONS METHODS HAVE SERIOUS DEFICIENCIES

There are no good, general transition correlations. The extreme complexity of the transition process requires that any technique make serious compromises. As previously discussed, transition is influenced by many parameters. Some parameters have a large effect and others have little or no effect. Several parameters appear to be competing for the dominant role, and, for a given situation, it is not always possible to predict the outcome. Even if one were successful in identifying the major parameters, it would not be possible to account for their individual effects in a transition correlation technique. Many effects become hidden in the empirical relationship. As long as the transition correlation is being applied to a configuration and flow condition similar to those of the data base used to establish the correlation, the hidden effects may not be greatly dissimilar. A problem exists, however, when one wants to apply a transition correlation to a configuration or flow condition unlike those of the data base. A change in the outcome of the competition of the various factors, or a change in the contribution of the various hidden effects, can greatly reduce the accuracy of the transition prediction. There is also the possibility that some unknown (or unexpected) phenomenon will come into play and drastically change the transition process (Morkovin refers to such unknown effects as "by-passes". The so-called "blunt body paradox" that was discovered in the 1950s is a good example).

One should always keep in mind that transition correlation techniques are always tailored to emphasize certain effects on a special class of configurations and flow conditions. Transition predictions should be made cautiously, with knowledge of how the criteria and prediction method was developed, how well the case in point corresponds to the pertinent data base, and with allowance that a hidden effect might cause a surprise. All transition predictions have an uncertainty associated with them. It would seem desirable to put an uncertainty band on any transition prediction to emphasize the degree of confidence in the prediction. Of course, the uncertainty can not be calculated, but it could represent an intuitive judgement as to how well transition was predicted.

5. WIND TUNNEL TRANSITION REYNOLDS NUMBERS ARE GENERALLY LOWER THAN CORRESPONDING FLIGHT TRANSITION REYNOLDS NUMBERS

Historically, the wind tunnel has been the major source of transition information. Often these wind tunnel data become the primary data base used to develop transition correlations and to establish transition criteria for flight. For most situations the transition Reynolds numbers obtained in wind tunnels are lower than corresponding flight transition Reynolds numbers. This is primarily the result of the strong freestream disturbance environment found in wind tunnels. It should be remembered that the differences between wind tunnel and flight transition Reynolds numbers are not the same throughout the Mach number range. The largest differences are generally at supersonic Mach numbers and the smallest differences are at subsonic and large hypersonic Mach numbers. Figures 2 and 3 illustrate these differences. Also, the specific configuration is a factor. In some cases, a transition parameter may be dominant enough to overshadow the difference in the freestream environment (e.g., bluntness or surface roughness). The wind tunnel transition Reynolds numbers obtained on the shuttle configuration were not much less than found in free flight.

Be cautious when using wind tunnel data to predict transition in flight. Many transition trends may be correctly reproduced in a wind tunnel, but the magnitude of the wind tunnel transition Reynolds numbers will generally be lower than expected in free flight.

6. SOMETIMES UNEXPECTED PHENOMENA CAN GREATLY REDUCE THE EXPECTED TRANSITION REYNOLD NUMBER

Most of our understanding of boundary layer stability and transition is derived from linear processes. In some situations disturbances can grow by some forcing mechanism and produce turbulence at Reynolds numbers even lower than those for the onset of linear disturbance growth. Morkovin[1,2] has referred to this process as a "by-pass", since transition has by-passed the linear processes. Reshotko[5] pointed out that much of our understanding has also been by-passed.

An example of by-pass transition occurs with high turbulence levels in the freestream. Reshotko[5] discussed the classic example of Poiseuille pipe flow. Another case was observed by Kendall[37] in wind tunnel experiments at a Mach number of 4.5. Disturbances of all frequencies were observed to grow monotonically larger in the region of a boundary layer extending from the flat plate leading edge to the predicted location of instability, i.e., in a region where linear stability theory indicated the boundary layer should be stable for all disturbance frequencies. This early growth of disturbances was attributed to the strong sound field generated by the turbulent boundary layer on the nozzle wall.

In any new transition situation there should be concern about unexpected transition behavior. The ballistic reentry transition problem of the 1950s should be remembered as an example of how wrong we can be. The blunt copper heatsink reentry vehicles were designed on the basis of maintaining a laminar boundary layer throughout reentry, all the way to impact. Having a laminar boundary layer to impact was then a logical conclusion, based upon knowledge available at that time. The stability theory of Lees[28] had indicated that wall cooling was very stabilizing. Van Driest[29] had made calculations which indicated after a certain cooling temperature ratio was exceeded, the boundary layer remained laminar for any Reynolds number. Steinberg's[38] V-2 flight had obtained laminar Reynolds numbers up to 90×10^6 (which is still believed to be the highest laminar Reynolds number ever reported), thus supposedly confirming the predictions of the stabilizing effects of cold walls. The heat sink reentry vehicle, in addition to having a highly cooled boundary layer, had a strong favorable pressure gradient which would be expected to provide additional stability. It was easy to conclude that the boundary layer would remain laminar until impact. Subsequent shock tube experiments* and flight experiments gave surprising results. It was found that a highly cooled blunt body does not maintain a laminar boundary layer to large Reynolds numbers, but, in fact, has very low transition Reynolds numbers. Transition on relatively smooth bodies typically occurred at length Reynolds numbers as low as 0.5×10^6 ($Re_\Theta \cong 300$). Surface roughness produced even lower transition Reynolds numbers. It is now thirty years later and an explanation of this blunt body paradox is still lacking.

Little is known about by-pass phenomena at this time. Therefore, for new transition situations, the transition predictor should consider the possible consequences of the low transition Reynolds numbers that might result if by-pass transition occurs.

---

* These results later appeared in the unclassified literature as Ref. 15.

7. THERE ARE UNIQUE FEATURES OF HYPERSONIC TRANSITION

It should not be assumed that supersonic and hypersonic transition characteristics are the same and that all supersonic transition data can be extrapolated to hypersonic Mach numbers. Hypersonic stability theory [4] and hypersonic stability experiments [22,26,33,37,39,40] have demonstrated there are unique features of hypersonic stability and transition. Several major features are briefly discussed below:

As predicted by Mack[4], the principle instabilities in a hypersonic boundary layer are second mode instabilities. Second mode disturbances are of high frequency, normally exceeding the frequency range of the principle supersonic disturbances (first mode). The hypersonic boundary layer is very selective in the frequency of the disturbances which are most amplified. There is evidence of a tuning effect of the boundary layer and the most amplified disturbances have a wavelength of approximately twice the boundary layer thickness. Second mode disturbances are not related to a specific frequency range, but can occur anywhere from relatively low frequencies (for "thick" boundary layers) to very high frequencies (for "thin" boundary layers). Situations which correspond to a change in boundary layer thickness, change the frequency of the second mode disturbances. For example, going to higher altitudes thickens the boundary layer and lowers the second mode disturbance frequencies. Cooling the wall thins the boundary layer and increases the second mode disturbance frequencies.

Reshotko [3,5,21,27] has often referred to transition as the consequence of the nonlinear response of that very complicated oscillator, the laminar boundary layer, to forcing disturbances. In a hypersonic boundary layer where the principal disturbances are expected to be of high frequency, the availability of high frequency forcing disturbances are a major issue. Thus, the influence of second mode disturbances on hypersonic boundary layer transition and therefore the characteristics of hypersonic transition are critically dependent upon the availability of suitable high frequency forcing disturbances.

We have grown accustomed to associating higher transition Reynolds numbers with increased wall cooling. This is appropriate for supersonic Mach numbers where the primary disturbances are first mode disturbances. The theory of Mack[4] has indicated that wall cooling has the opposite effect, a destabilizing effect, on the stability of a hypersonic boundary layer. Limited hypersonic stability experiments[23, 33] have confirmed the destabilizing effect of wall cooling. For hypersonic situations where the major disturbances are not second mode disturbances, the effects of wall cooling are not clear.

Several figures from References 22 and 39 are included to illustrate some of the characteristics of hypersonic boundary layer disturbances. Fig. 18 shows the fluctuation spectra at the location of peak energy in the boundary layer in a pictorial format to illustrate the growth of disturbances in a hypersonic laminar boundary layer. The large disturbances which grew in the frequency range from about 70 to 150 kHZ are second mode disturbances. Even though the boundary layer disturbances had grown to a relatively large amplitude by the end of the model, the boundary layer still had the mean flow characteristics of a laminar boundary layer. Fig. 19 contains the same data as shown in the previous figure, with spectral data from several stations overlayed to better illustrate the disturbance frequencies. The first and second mode fluctuations are merged. The first mode corresponds to the lower frequency fluctuations which show an increase in amplitude without any special selectivity in frequency of the disturbances which are amplified. These disturbances are similar to the Tollmien-Schlichting instability of incompressible flow. The large increase in fluctuation amplitude in the frequency range of about 70 to 150 kHZ are second mode disturbances. As the boundary layer grows, the second mode disturbance peaks shift to lower frequencies, illustrating the tuning effect of the boundary layer. Fig. 20 is a pictorial view showing the spectral density variations through the boundary layer. Fig. 20a is a view from outside the boundary layer, looking in and Fig. 20b is a view from the surface, looking out. It can be seen that the disturbances did not grow in the inner half of the boundary layer, the maximum disturbance growth occurred high in the boundary layer (at approximately 88% of the boundary layer thickness), and disturbances extended well beyond the defined boundary layer edge. Fig. 21 illustrates the relationship between the wavelength of the major disturbances and the boundary layer thickness. As a means of comparison, the major first mode disturbances in lower speed flows have a much longer wave length, typically being several times the boundary layer thickness.

Mack[4] has warned us that parameters such as wall temperature, pressure gradient, and mass addition or removal may not affect second model disturbances in the same manner as they did first mode disturbances. We have some experimental evidence that this is true for wall temperature. There are no experimental results available to evaluate the affect of other parameters. This is another area where we could find some surprises.

8. THE LENGTH OF THE TRANSITION REGION VARIES

As a rule-of-thumb, it has been customary in the past to assume that the length of the transition region was the same as the length of the laminar region. The end of transition is not as well documented as the onset; however, there is a reasonable amount of data to support this conclusion. For example, the sharp cone and sharp plate correlations of Masaki and Yakura[41] and the extensive work of Pate[42] support this reasoning. Pate found $(Re_{XT})_B/(Re_{XT})_E \cong 0.5$ for a range of local Mach numbers from 3 to 8. There may be some variations in the reported transition lengths due to the method of detecting transition onset. The location of transition onset has been found to vary depending upon the method of detection; whereas, the end of transition was essentially independent of the method used. For example, transition onset detected optically is consistently further downstream than onset detected by heat transfer rate or surface total pressure. These findings prompted Pate to make his correlations based upon the end of transition, rather than onset. Harvey and Bobbitt[43] have reported that in low noise wind tunnels and free flight the transition region can be much shorter than the laminar region, with $(Re_{XT})_B/(Re_{XT})_E$ varying from about 0.5 to 0.9. Most free flight experiments have added uncertainties due to the inability to control the flow conditions and vehicle altitude, coupled with more restrictions on vehicle instrumentation. An exception was the carefully controlled flight experiments of Dougherty and Fisher[7]. A 5-deg. half angle cone, which had been extensively tested in transonic and supersonic wind tunnels, was mounted on the nose boom of an F-15 aircraft and flight tested. The same instrumentation, primarily a surface pitot probe, detected transition both in flight and in the wind tunnels. The flight experiments, up to a Mach number of 2.0, measured a very short transition region, with $(Re_{XT})_B/(Re_{XT})_E$ being between 0.8 and 0.9. Mach 6 wind tunnel experiments[18] (see Figures 10 and 12), on a 8-deg half angle cone with both a sharp tip and small nosetip bluntness, found X_{TB}/X_{TE} to be approximately 0.75. With larger nosetip bluntness, which produced early frustum transition, there was typically a very long transition region. Usually the transition region extended to the end of the model so that the end of transition could not be measured, with the transition length being several times as long as the laminar length. The Reentry F flight test data showed large variations in the length of the transition region. At 84,000 feet, $(Re_{XT})_B/(Re_{XT})_E = 0.64$ and at 60,000 feet, the value reduced to 0.009. These results very likely reflect the coupling of several effects and are difficult to interpret.

It can be seen that the length of a transition region to be expected in hypersonic free flight is not well defined and predictable. The Reentry F flight results would support long transitional regions; whereas, several other results indicated that short transitional regions should be expected. There is clearly a large uncertainty associated with a prediction of the transition length.

9. CALCULATIONS OF BOUNDARY LAYER PROPERTIES ARE IMPORTANT

Much of the available hypersonic transition data were obtained 20 or more years ago. The techniques used to generate the boundary layer properties for the analyses of these results were often primitive by today's standards. The boundary layer properties are an important element in the interpretation and analysis of transition results. The uncertainty of an author's boundary layer calculations are often overlooked when studying his results and comparing his data with the data of others. For both old and new results, attention should be given to how the flow field properties were obtained.

PART II: COMMENTS ON SEVERAL TRANSITION PREDICTION METHODS

1. $Re_{\theta T}/Me$ = CONSTANT

One of the most commonly used transition prediction methods is to use $Re_{\theta T}/Me$ = constant. This technique was used for the Space Shuttle, and this prior usage has seemed to make it a prime candidate for future transition predictions. The fact that it worked reasonably well for the Shuttle was due to the uniqueness of that situation and this should not be interpreted as verification of the technique in general. The Shuttle's very blunt nosetip, high angle of attack, rough surface, and locally supersonic flow (with little variation) always produced relatively low transition Reynolds numbers which were not much larger than obtained in wind tunnels. It can easily be shown Re_{θ}/Me = constant should not be expected to have a general application. Fig. 22 schematically shows the trend of transition Reynolds number vs Mach number variation for sharp cones. When a cone with nosetip bluntness is considered, a whole family of curves result, with a separate curve for each freestream Mach number. When we say Re_{θ}/Me = constant, we are trying to represent all of these data by a single slope. There is only one region where a single slope can be expected to provide a reasonable representation of the data. For a sharp cone and $Me > 8$, a slope of about 100 seems to be reasonable. Note that for subsonic Mach numbers the constant can exceed 1000. Therefore, for Mach numbers up to 8, the constant is varying by a factor of 10. When consideration is given to entropy layer effects generated by a nosetip, there is no region where a constant slope has any credibility. The best that can be done is to use some average slope. The fact that Space Shuttle flight transition data gave a slope in the range of 200-400 at $Me \cong 2$ is of no value in predicting transition on a hypersonic vehicle with large local Mach numbers.

It should be remembered that Re_θ is proportional to $(Re_x)^{\frac{1}{2}}$. Therefore, plots of Re_θ, and the variations in Re_θ, must be viewed in this perspective. It was thought to be informative to show a comparison of Re_θ and Re_x. Fig. 23 shows approximate calculations for sharp cones. Note the large variations in Re_x at large local Mach numbers that result from changes in the Re_θ/M_e constant. For example, at $M_e = 15$:

Re_θ/Me	Re_x
100	36.9×10^6
200	148×10^6
300	332×10^6
400	590×10^6

Considering that the Reentry F flight data indicated a sharp cone transition Reynolds number of approximately 40×10^6, which corresponds to an $Re_\theta/_{Me}$ just over 100, there seems to be no rationale for using large values of $Re_\theta/_{Me}$ for this case.

Using $Re_\theta/_{Me}$ = constant, and using the same constant for a range of local Mach numbers, is not likely to result in good transition predictions.

2. $Re_{\theta T}$ vs X/R_N

Probably the most extensive transition correlation study ever made was performed by Martellucci and associates. Some of these results are presented in Ref. 44. They considered approximately 200 reentry vehicle ($M_\infty \cong 20$) cases and selected those which met the following criteria:

a. Small angles of attack at transition onset, $\alpha/\theta_c \leq 0.1$

b. The trajectory could be determined

c. Sphere - cone configurations

d. On-board sensors

e. Redundant transition altitude sensors

This resulted in the consideration of 72 reentry vehicles and 149 data points. In order to obtain a consistent set of boundary layer properties they performed the following calculations:

a. Utilization of engineering methods to determine thermochemical shape change of ablative nosetips throughout reentry - the results of which were used as inputs to the inviscid flow field and boundary layer codes.

b. A numerical solution of the inviscid shock layer for axisymmetric bodies, to provide shock shape and surface pressure distributions.

c. A numerical solution of the heat conduction equation to define in-depth material response, frustum ablation, and surface temperature characteristics.

d. A numerical implicit finite difference solution of the boundary layer equations which included mass addition effects.

The resulting data were correlated against over 50 different transition correlation techniques ($Re_\theta/_{Me}$ = constant, was one). A significant, although not surprising, result was that none of the correlation techniques did a good job of correlating the data. Re_θ vs X_T/R_N correlations were considered to be the best and further improvements could be made by using sub-sets of data for like heat shield materials. Fig. 24 (from Ref. 44) shows some of the results. Like all transition correlations, many effects are not accounted for. This correlation applies only to Mach 20 reentry vehicles and should not be used, as is, for other Mach numbers since the relationship is Mach number dependent. Bluntness effects are only partially included, but as long as only slender reentry vehicles with small nosetip bluntness are considered, bluntness effects are nearly similar. That is, using Rotta's[12] similarity approach for highly cooled sphere-cones, the boundary layer properties within the entropy layer resulting from the nosetip are a function of $\dfrac{S/R_N}{K(Re_\infty/FT,\ R_N)^{1/3}}$

where the constant K is primarily a function of cone angle and Mach number and can be obtained from Fig. 6. Thus, for situations where $K(Re_\infty/FT,\ R_N)^{1/3}$ does not vary significantly, S/R_N, by itself, adequately accounts for the variation of boundary layer properties within the entropy layer. Note, also, that it is the product of these terms that is important, not their individual values. Thus, if the freestream unit Reynolds number is decreased an order of magnitude (increasing altitude by approximately 50 K feet) and the nosetip radius is increased an order of magnitude, the entropy layer, in terms of S/Rn is unchanged.

This $Re_{\theta T}$ vs X/R_N transition correlation was not meant to be a general correlation and should not be used as such. Like all correlations, it should be used only where it is appropriate.

3. e^N Method

The most common analytical approach to predicting transition follows the method of Smith[45] and Van Ingen[46]. Linear stability theory is utilized to calculate amplitude ratios. Transition is presumed to occur with the earliest attainment of some preassigned amplitude ratio, usually expressed as e^N. There is no theoretical justification for the use of this method to predict transition, since all it does is compute an amplitude ratio (A/Ao). It ignores the environment (A_0) and the actual transition process. The value of N must be input, based upon available experimental data, and transition is predicted to occur when N reaches the preassigned value. Within the limits of the theory being used, it can be used to study the influence of various parameters on transition. This method has been used for subsonic flow and NASA Langley has automated the calculation procedure with codes called SALLY (incompressible) and COSAL (compressible).

Considerable additional work is required in order to apply this method to hypersonic, three-dimensional configurations. The theory must include the higher instability modes (Mack modes) and be able to treat entropy layers, pressure gradients, three-dimensional effects, and real gas effects. Assuming that these theoretical advances will be made, experimental verification of these new results will be required before the method can be confidently used. As with any new analytical tool, experimental verification is an essential part of the process. The magnitude of this overall task can be illustrated by pointing out that it has never been verified that current stability theory can identify the most unstable disturbance frequencies and calculate their growth rates even for the simple case of flow over a sharp cone at zero angle of attack in a hypersonic, perfect gas.

Although it is currently not possible to confidently predict hypersonic transition by analytical methods, this is clearly the goal for future predictions. Analytical prediction methods have the potential of providing the transition predictor with a more general technique which can account for many of the physical aspects of the flow. It will not only be possible to investigate the combined effects of many parameters, but to isolate various effects for parametric studies.

PART III: SOME THOUGHTS ON HOW TO PREDICT HYPERSONIC TRANSITION IN 1987

As stated previously, there is no good general technique for predicting hypersonic transition. However, it should be possible to make a better prediction than can be obtained from the relationship, Re_θ/Me = constant. Whatever the prediction method being used, the main message is to try to understand the method and be aware of its limitations and the uncertainty of the prediction. Following are some comments for consideration in making transition predictions in 1987.

Hypersonic configurations, through necessity, will have some degree of nosetip bluntness. Due to the fact that nosetip transition Reynolds numbers are very low, possibly being two orders of magnitude less than frustum transition Reynolds numbers, it is necessary to consider nosetip transition independently from frustum transition. This basically requires a calculation of the Reynolds number at the sonic point, along with an allowance for the surface roughness at the sonic point. It is suggested that three regions of a configuration be considered and a separate transition criterion applied to each region. These regions are a) nosetip, b) early frustum, and c) frustum.

1. Nosetip: Determine if transition will occur on the nosetip. If transition does occur on the nosetip, all flow downstream, progressing from that region of the nosetip, should be transitional or turbulent. Nosetip transition is insensitive to freestream Mach number and very dependent upon nose tip radius and surface roughness. Nosetip transition has been

investigated quite extensively and a number of transition correlations are available. Fig. 8 contains some of the results of PANT[16] and Demetriades[17]. Re_θ calculated at the sonic point, is shown as a function of roughness height and boundary layer parameters. For a "smooth" nosetip, Re_θ's greater than about 300 can result in transition on the nosetip. A rough nosetip produces transition at lower Reynolds numbers. Ref. 47 contains a review and evaluation of nosetip transition experiments.

2. Early Frustum: Early frustum transition is a subject which has only recently been identified. The transition experiments reported in Ref. 9 clearly identified the early cone frustum as a region with its own transition criteria. This region, which extended for several nose radii down the frustum, had very low transition Reynolds numbers. It was determined that transition on the early part of the frustum could be related to conditions on the nosetip. Early frustum transition could be related to the Reynolds number at the sonic point and the nosetip surface roughness, analogous to the nosetip transition criteria. Therefore, calculations of Re_θ at the nosetip sonic point can also be used to predict early frustum transition. For a sphere-cone at a Mach number of 6, Re_θ's of 120, or greater, at the sonic point of a smooth nosetip produced transition on the early portion of the frustum. That is, for Re_θ's at the sonic point of less than 120, both the nosetip and the early portion of the frustum had a laminar boundary layer. For Re_θ's from 120 to about 300, the nosetip had a laminar boundary layer and transition occurred on the early region of the frustum. For Re_θ's of about 300 or greater, transition occurred on the nosetip. Fig. 8 gives a criterion for both early frustum transition and nosetip transition. Unfortunately, not enough information is known about early frustum transition to determine the generality of these results. It

appears that the results are sensitive to the favorable pressure gradient. Increasing the pressure gradient, as would result from increasing the freestream Mach number, is expected to increase the threshold value of Re_θ above 120. Likewise, decreasing the pressure gradient is expected to reduce the threshold value.

3. Frustum: If the frustum of the configuration has adverse pressure gradients, such as associated with a ramp, the frustum should be separated into two regions for separate considerations - the zero pressure gradient region and the adverse pressure gradient region.

a. Zero Pressure Gradient Region: As a minimum for this region, consideration should be given to Mach number, entropy layer, and three dimensional effects. Other effects, such as unit Reynolds number, mass addition, wall temperature, real gases, the environment, and surface roughness should be considered if one has some basis for making an estimate of their effect. This consideration could be in a form of biasing the final transition Reynolds number, either upward or downward.

One possible approach would be to estimate the transition Reynolds number for a sharp configuration, with consideration for Mach number and cross flow effects. Data such as found in Fig. 3 and 9 can be helpful in establishing this number. Next consider how the transition Reynolds number varies from the sharp cone value when it occurs within the entropy layer. Even a small amount of nosetip bluntness can generate entropy layer effects which extend for great distances downstream. Fig. 25 illustrates this point, with calculations of entropy layer swallowing lengths obtained from Rotta's similarity ($X = 3\ X_{SW}$

was considered to be the location where the effects of the entropy layer did not significantly influence transition). Since the extent of the entropy layer will normally be large, its effect on the transition Reynolds number should be included. Again there is only limited information available to make this judgement. The similarity of Mach 6 wind tunnel data[9] and Mach 20 flight data[13] would suggest that the percentage change in transition Reynolds number through the entropy layer affected region is not greatly affected by freestream Mach number. Fig. 26 illustrates the ratio of local transition Reynolds number to the sharp cone transition Reynolds number variation through the entropy layer affected region. In the interim period, this figure may be used to estimate transition Reynolds number variations through this region.

b. Adverse Pressure Gradient Region: Based upon available results, any region of "significant" adverse pressure gradient would be expected to have a much lower transition Reynolds number than zero-pressure gradient regions. Unfortunately, not enough is known about the effects of adverse pressure gradients on hypersonic transition to be of much help. This is an area where there is great need for new experimentation. In the interim, one can only make a guess as to what the transition Reynolds number should be in an adverse pressure gradient region. When one parameter has a dominating effect on transition, resulting in low transition Reynolds numbers, the influence of other parameters are minimized. Therefore, the effects of Mach number, entropy layer, and cross flow may be small in regions of a dominating adverse pressure gradient. Laminar boundary layers are more susceptible to boundary layer separation than turbulent boundary layers. The free shear layers associated with separated flow are more unstable than attached flows and are expected to produce low transition Reynolds numbers. Until more information is available, a rough estimate of the transition Reynolds number in an adverse pressure gradient region may be made by assuming a transition criteria based upon some percentage of the zero pressure gradient value.

***

In future years, as more hypersonic transition data becomes available, we can improve our empirical techniques. Our ultimate goal is to predict hypersonic transition by analytical methods. In the near term, techniques like the e^N method can be used. Some day we will predict transition through solutions of the three-dimensional, time-dependent, Navier-Stokes equations.

REFERENCES

1. Morkovin, M. V., "Critical Evaluation of Transition From Laminar to Turbulent Shear Layers with Emphasis on Hypersonically Traveling Bodies", AFFDL TR-68-149, March 1969.

2. Morkovin, M. V., "Instability, Transition to Turbulence and Predictability", AGARDograph No. 236, July 1978.

3. Reshotko, Eli, "Boundary Layer Stability and Transition", Annual Review of Fluid Mechanics, Vol. 8, pp 311-350, 1976.

4. Mack, L. M., "Boundary Layer Linear Stability Theory", AGARD Report No. 709, June 1984 (Also, see AIAA Journal, Vol. 13, No. 3, pp. 278-289, March 1975).

5. Reshotko, Eli, "Stability and Transition, How Much Do We Know?", paper presented at Tenth U. S. National Congress of Applied Mechanics, The University of Texas at Austin, Austin, Texas, June 1986.

6. White, C. O., "Boundary Layer Transition for Sharp and Slight Blunted Cones Under Hypersonic Entry Conditions", Philco-Ford Corp. Mechanical Eng. TN 110, Oct 1966.

7. Dougherty, N. S., Jr., and Fisher, D. F., "Boundary-Layer Transition Correlations on a Slender Cone in Wind Tunnels and Flight for Indications of Flow Quality", AEDC-TR-81-26, Feb 1982 (also AIAA-80-0154, Jan 1980).

8. Beckwith, I. E., "Development of a High Reynolds Number Quiet Tunnel for Transition Research", AIAA Journal, Vol. 13, No. 3, pp. 300-306, March 1975.

9. Stetson, K. F., "Nosetip Bluntness Effects on Cone Frustum Boundary Layer Transition in Hypersonic Flow", AIAA Paper No. 83-1763, July 1983.

10. Muir, J. R. and Trujillo, A. A., "Experimental Investigation of the Effects of Nose Bluntness, Free-Stream Unit Reynolds Number, and Angle of Attack on Cone Boundary Layer Transition at a Mach Number of 6", AIAA Paper No. 72-216, Jan 1972.

11. Stetson, K. F. and Rushton, G. H., "Shock Tunnel Investigation of Boundary Layer Transition at M=5.5", AIAA Journal, Vol. 5, pp. 899-906, May 1967.

12. Rotta, N. R., "Effects of Nose Bluntness on the Boundary Layer Characteristics of Conical Bodies at Hypersonic Speeds", NYU-AA-66-66, Nov 1966 (Also, Astronautics Acta, Vol. 13, 1968, pp. 507-516).

13. Wright, R. L. and Zoby, E. V., "Flight Boundary Layer Transition Measurements on a Slender Cone at Mach 20", AIAA Paper No. 77-719, June 1977.

14. Johnson, C. B., Stainback, P. C., Wicker, K. C., and Boney, L. R., "Boundary-Layer Edge Conditions and Transition Reynolds Number Data for a Flight Test at Mach 20 (Reentry F)", NASA TM-X-2584, July 1972.

15. Stetson, K. F., "Boundary Layer Transition on Blunt Bodies with Highly Cooled Boundary Layers", J. A. S., Vol. 27, pp. 81-91, Feb 1960 (Also, IAS Report No. 59-36, Jan 1959).

16. Anderson, A. D., "Interim Report, Passive Nosetip Technology (PANT) Program, Vol. X, Appendix, Boundary Layer Transition on Nosetips with Rough Surfaces", SAMSO-TR-74-86, Jan 1975.

17. Demetriades, A., "Nosetip Transition Experimentation Program, Final Report, Vol. II", SAMSO-TR-76-120, July 1977.

18. Stetson, K. F., "Mach 6 Experiments of Transition on a Cone at Angle of Attack", Journal of Spacecraft and Rockets, Vol. 19, No. 5, Sept-Oct 1982, pp. 397-403.

19. Potter, J. L., "Boundary-Layer Transition on Supersonic Cones in an Aeroballistic Range", AIAA Journal, Vol. 13, No. 3, March 1975, pp. 270-277.

20. Potter, J. L., "The Unit Reynolds Number Effect on Boundary Layer Transition", Dissertation submitted in partial fulfillment of the requirements for the degree of Doctor of Philosophy, Vanderbilt Univ., May 1974.

21. Reshotko, E., "Stability Theory as a Guide to the Evaluation of Transition Data", AIAA Journal, Vol. 7, No. 6, June 1969, pp. 1086-1091.

22. Stetson, K. F., Thompson, E. R., Donaldson, J. C., and Siler, L. G., "Laminar Boundary Layer Stability Experiments on a Cone at Mach 8, Part 4: On Unit Reynolds Number and Environmental Effects", AIAA Paper No. 86-1087, May 1986.

23. Schubauer, G. B. and Skramstad, H. K., "Laminar Boundary Layer Oscillations and Transition on a Flat Plate", NASA Report No. 909, 1948.

24. Wells, C. D., Jr., "Effects of Freestream Turbulence on Boundary Layer Transition", AIAA Journal, Vol. 5, No. 1, pp. 172-174, Jan 1967.

25. Spangler, J. G. and Wells, C. S., Jr., "Effects of Free Stream Disturbances on Boundary Layer Transition", AIAA Journal, Vol. 6, No. 3, pp. 543-545, March 1968.

26. Stetson, K. F., Thompson, E. R., Donaldson, J. C. and Siler, L. G., "Laminar Boundary Layer Stability Experiments on a Cone at Mach 8, Part 3: Sharp Cone at Angle of Attack", AIAA Paper No. 85-0492, Jan. 1985.

27. Reshotko, E., "Environment and Receptivity", AGARD Report No. 709, pp. 4-1 to 4-11, 1984.

28. Lees, L., "The Stability of the Laminar Boundary Layer in a Compressible Fluid", NASA Report No. 876, 1947.

29. Van Driest, E. R., "Calculations of the Stability of the Laminar Boundary Layer in a Compressible Fluid on a Flat Plate with Heat Transfer", JAS, Vol. 19, No. 12, pp. 801-812, 828, Dec. 1952.

30. Jack, J. R., Wisniewski, R. J. and Diaconis, N. S., "Effects of Extreme Surface Cooling on Boundary Layer Transition", NASA TN 4094, Oct. 1957.

31. Sheetz, N. W., Jr., "Free-Flight Boundary Layer Transition Investigation at Hypersonic Speeds", AIAA Paper No. 65-127, Jan. 1965.

32. Van Dreist, E. R., and Boison, J. C., "Experiments on Boundary Layer Transition at Supersonic Speeds", JAS, Vol. 24, pp. 885-889, 1957.

33. Demetriades, A., "New Experiments on Hypersonic Boundary Layer Stability Including Wall Temperature Effects", Proceedings of the Heat Transfer and Fluid Mechanics Institute, pp. 39-54, 1978.

34. Boudreau, A. H., "Artificially Induced Boundary Layer Transition on Blunt-Slender Cones at Hypersonic Speeds", Journal of Spacecraft and Rockets, Vol. 16, pp. 245-251, July - Aug. 1979.

35. Martellucci, A., Neff, R. S., and Rittenhouse, C., "Mass Addition Effects or Vehicle Forces and Moments - Comparison Between Theory and Experiment", General Electric Document 69SD934, Sept. 1969.

36. Beckwith, I. E., and Bertram, M. H., "A Survey of NASA Langley Studies on High-Speed Transition and the Quiet Tunnel", NASA TM X-2566, July 1972.

37. Kendall, J. M., "Wind Tunnel Experiments Relating to Supersonic and Hypersonic Boundary Layer Transition", AIAA Journal, Vol. 13, No. 3, pp. 290-299, March 1975.

38. Sternberg, J., "A Free Flight Investigation of the Possibility of High Reynolds Number Supersonic Laminar Boundary Layers", Journal Aero. Sci., Vol. 19, Nov. 1952.

39. Stetson, K. F., Thompson, E. R., Donaldson, J. C., and Siler, L. G., "Laminar Boundary Layer Stability Experiments on a Cone at Mach 8, Part 1: Sharp Cone", AIAA Paper No. 83-1761, July 1983.

40. Stetson, K. F., Thompson, E. R., Donaldson, J. C., and Siler, L. G., "Laminar Boundary Layer Stability Experiments on a Cone at Mach 8, PArt 2: Blunt Cone", AIAA Paper No. 84-0006, Jan. 1984.

41. Masaki, M. and Yakura, J. K., "Transitional Boundary Layer Considerations for the Heating Analysis of Lifting Re-Entry Vehicles", Journal of Spacecraft and Rockets, Vol. 6, No. 9, pp. 1048-1059, Sept. 1969.

42. Pate, S. R., "Dominance of Radiated Aerodynamic Noise on Boundary Layer Transition in Supersonic-Hypersonic Wind Tunnels, Theory and Application", AEDC-TR-77-107, March 1978.

43. Haravey, W. D. and Bobbitt, P. J., "Some Anomalies Between Wind Tunnel and Flight Transition Results, "AIAA Paper No. 81-1225, June 1981.

44. Berkowitz, A. M., Kyriss, C. L. and Martellucci, A., "Boundary Layer Transition Flight Test Observations", AIAA Paper No. 77-125, Jan. 1977.

45. Smith, A. M. O. and Gamberoni, N., "Transition, Pressure Gradient and Stability Theory", Douglas Aircraft Co. Report No. ED 26388, 1956.

46. Van Ingen, J. L., "A Suggested Semi-Empirical Method for the Calculation of the Boundary Layer Transition Region", Dept. of Aero. Eng., Delft, Reports VTH-71 and VTH-74, 1956.

47. Batt, R. G., and Legner, H. H., "A Review of Roughness Induced Nosetip Transition", AIAA Paper No. 81-1223, June 1981.

APPENDIX

FLIGHT

TRANSITION

RESULTS

REENTRY VEHICLE

TRANSITION RESULTS

FROM REF. 44

TABLE 2. LOCAL TRANSITION PROPERTIES

DATA POINT	RN (IN)	θ_c (DEG)	NOSE MAT.	FRUST. MAT.	HBAR	U(INF) (FT/SEC)	S (IN)	TW (DEG R)	PE (LBF/FT2)	HE (BTU/LBM)	ME	Re_{xT}	Re_{θ}	REDST
1	0.18	6.0	GRB	BE	0.75	2.166E 04	40.39	8.728E 02	6.904E 02	8.780E 02	7.31	7.170E 06	8.300E 02	7.000E 03
2	0.18	6.0	GRH	TFE	0.95	2.197E 04	38.96	1.796E 03	2.677E 02	3.150E 02	12.47	1.250E 07	2.790E 03	3.820E 04
3	0.10	5.0	GRB	BE	1.00	1.976E 04	144.67	5.024E 02	1.286E 02	2.000E 02	14.73	4.943E 07	1.770E 03	5.400E 04
4	0.18	8.4	GRB	BE	1.25	2.247E 04	140.30	6.479E 02	1.308E 02	3.875E 02	11.65	1.555E 07	1.130E 03	1.860E 04
5	0.18	6.0	GRB	BE	0.65	1.796E 04	40.42	9.846E 02	8.034E 02	6.600E 02	7.21	1.034E 07	1.044E 03	8.720E 03
6	0.68	6.0	GRB	BE	0.60	1.872E 04	36.17	8.572E 02	7.056E 02	2.972E 03	3.06	1.450E 06	4.400E 02	5.300E 02
7	0.25	8.0	GRB	SP	1.17	2.250E 04	101.28	1.996E 03	1.675E 02	3.367E 02	12.30	1.840E 07	2.470E 03	4.840E 04
8	0.25	6.0	TFE	TFE	1.16	2.275E 04	101.00	1.800E 03	1.599E 02	3.050E 02	13.13	1.900E 07	1.850E 03	4.780E 04
9	2.25	6.0	PH	BE	0.95	1.570E 04	47.30	6.764E 02	1.093E 02	1.717E 03	3.67	4.040E 05	6.220E 02	6.920E 02
10	2.25	6.0	PH	BE	1.00	1.970E 04	47.25	6.525E 02	1.276E 02	3.129E 03	3.76	3.260E 05	4.450E 02	3.840E 02
11	2.25	6.0	GRB	BE	0.50	1.600E 04	47.07	1.092E 03	9.977E 02	2.302E 03	3.36	2.530E 06	5.190E 02	7.100E 02
12	2.25	6.0	PH	BE	0.69	1.980E 04	45.44	7.370E 02	2.168E 02	3.610E 03	3.45	4.430E 05	3.900E 02	3.180E 02
13	2.35	6.0	GRB	BE	0.54	1.675E 04	51.12	9.293E 02	6.716E 02	2.528E 03	3.43	2.360E 06	4.150E 02	6.090E 02
14	2.25	6.0	PH	BE	0.90	1.950E 04	47.19	6.570E 02	2.001E 02	3.290E 03	3.60	4.060E 05	5.060E 02	5.080E 02
15	0.25	6.0	GRH	BE	1.17	2.240E 04	102.87	5.923E 02	1.061E 02	3.240E 02	12.60	1.946E 07	1.190E 03	2.240E 04
16	0.25	10.0	GRB	BE	1.11	2.145E 04	81.03	8.236E 02	3.011E 02	3.620E 02	11.15	2.046E 07	1.310E 03	2.030E 04
17	0.25	10.0	GRB	BE	1.11	2.145E 04	81.03	8.236E 02	3.011E 02	3.620E 02	11.15	2.046E 07	1.310E 03	2.030E 04
18	0.25	4.5	GRB	CP	0.64	1.645E 04	64.47	1.997E 03	4.742E 02	4.229E 02	8.00	2.140E 07	1.910E 03	1.912E 04
19	0.25	7.2	PH	CP	0.86	2.240E 04	44.70	1.659E 03	7.110E 02	6.766E 02	9.06	1.233E 07	1.080E 03	1.180E 04
20	0.38	8.6	GRB	GR	0.64	1.964E 04	27.62	3.199E 03	1.906E 03	2.090E 03	4.92	4.350E 06	1.270E 03	2.890E 03
21	0.18	8.4	PH	CP	1.22	2.240E 04	139.55	1.029E 03	1.392E 02	3.716E 02	11.80	1.800E 07	1.240E 03	2.120E 04
22	0.25	10.0	GRB	PH.6	1.06	2.200E 04	77.05	1.092E 03	4.009E 02	3.920E 02	11.20	2.540E 07	1.930E 03	3.090E 04
23	0.25	8.0	GRB	SP	1.06	2.235E 04	101.27	1.461E 03	2.775E 02	3.100E 02	12.84	3.460E 07	2.980E 03	5.900E 04
24	0.50	8.6	PH	SP	0.82	2.200E 04	38.50	3.062E 03	9.804E 02	1.595E 03	6.23	4.780E 06	1.330E 03	4.380E 03
25	0.38	8.6	PH	SP	0.74	2.120E 04	40.14	3.633E 03	1.307E 03	1.120E 03	6.90	9.500E 06	2.690E 03	9.220E 03
26	0.50	7.2	PH	3DQP	0.90	2.235E 04	50.97	1.248E 03	5.038E 02	7.657E 02	8.45	7.900E 06	2.340E 03	1.060E 04
27	1.50	8.3	PH	QP	1.12	2.200E 04	129.14	1.240E 03	2.137E 02	8.590E 02	7.96	7.490E 06	2.190E 03	9.260E 03
28	1.25	9.0	GRB	CP	0.30	2.260E 04	63.10	2.446E 03	1.201E 03	3.997E 03	3.92	2.650E 06	8.830E 02	2.230E 03
29	0.75	6.3	GRB	CP	0.75	2.202E 04	72.40	2.300E 03	6.974E 02	3.137E 03	4.59	2.740E 06	8.080E 02	2.490E 03
30	1.50	6.3	GRB	3DQP	0.78	2.260E 04	64.10	1.893E 03	4.606E 02	4.557E 03	3.62	8.530E 05	5.680E 02	9.470E 02
31	2.04	5.9	GRB	3DQP	0.93	2.303E 04	56.50	2.207E 03	2.098E 02	4.970E 03	3.59	3.200E 05	3.570E 02	4.380E 02
32	0.25	8.6	GRB	SP	0.75	2.117E 04	39.50	4.473E 03	1.256E 03	2.058E 03	5.41	4.030E 06	9.060E 02	4.280E 03
33	1.50	6.6	GRH	SP	0.70	2.004E 04	34.20	4.973E 03	9.451E 02	3.910E 03	3.24	9.680E 05	5.320E 02	9.880E 02
34	0.50	9.0	GRB	GR	0.39	1.380E 04	47.00	2.522E 03	3.546E 03	1.507E 03	3.40	1.050E 07	1.480E 03	4.030E 03
35	0.25	22.0	GRB	BE	1.17	2.239E 04	38.20	9.366E 02	1.063E 03	1.694E 03	6.27	4.380E 06	7.450E 02	2.700E 03
36	0.25	22.0	GRB	BE	1.19	2.241E 04	38.10	9.061E 02	9.693E 02	1.697E 03	6.26	4.000E 06	7.140E 02	2.560E 03
37	0.25	22.0	GRB	BE	1.18	2.240E 04	38.20	9.960E 02	1.039E 03	1.695E 03	6.27	4.280E 06	7.360E 02	2.650E 03
38	0.25	8.0	GRB	BE	1.22	2.162E 04	170.00	7.599E 02	1.251E 02	3.190E 02	12.37	2.280E 07	1.300E 03	2.530E 04
39	0.10	8.0	GRH	SP	1.20	2.259E 04	169.00	1.960E 03	1.465E 02	3.550E 02	12.25	2.400E 07	1.500E 03	2.970E 04
40	0.10	8.0	GRH	BE	1.25	2.259E 04	171.00	6.616E 02	1.164E 02	3.540E 02	12.21	1.910E 07	1.210E 03	2.180E 04
41	0.25	8.0	GRB	CP	0.99	2.078E 04	83.20	2.044E 03	3.356E 02	3.390E 02	11.44	2.620E 07	1.670E 03	3.330E 04
42	0.64	5.9	GRB	QP	0.48	1.733E 04	60.50	2.765E 03	1.389E 03	2.474E 03	3.68	4.120E 06	9.430E 02	2.290E 03
43	0.64	5.9	GRB	QP	0.64	1.549E 04	65.50	2.340E 03	5.918E 02	1.561E 03	4.05	2.890E 06	7.760E 02	2.330E 03
44	1.20	5.9	GRB	QP	0.59	1.510E 04	62.00	1.394E 03	5.907E 02	1.843E 03	3.57	2.160E 06	6.760E 02	1.430E 03
45	1.80	7.0	GRH	CP	0.65	2.159E 04	54.80	2.375E 03	9.221E 02	4.366E 03	3.37	1.390E 06	6.850E 02	9.280E 02
46	1.80	7.0	GRB	CP	0.66	2.169E 04	54.80	2.365E 03	8.875E 02	4.413E 03	3.40	1.320E 06	6.720E 02	9.130E 02
47	2.35	6.0	GRB	BE	0.77	1.881E 04	50.10	9.066E 02	3.469E 02	3.271E 03	3.47	7.250E 05	4.510E 02	5.390E 02
48	0.25	8.0	GRB	SP	0.93	2.258E 04	101.00	2.616E 03	5.198E 02	3.890E 02	11.68	4.430E 07	2,380E 03	4.880E 04
49	0.25	8.0	GRB	BE	1.09	2.281E 04	103.00	7.213E 02	2.437E 02	3.020E 02	13.30	3.050E 07	1.480E 03	3.280E 04
50	0.25	8.0	GRB	SP	1.05	2.340E 04	101.00	2.495E 03	3.218E 02	3.130E 02	13.42	3.860E 07	2.050E 03	5.180E 04

TABLE 2. LOCAL TRANSITION PROPERTIES (CONT.)

DATA POINT	RN (IN)	θ_c (DEG)	NOSE MAT.	FRUST. MAT.	HBAR	U(INF) (FT/SEC)	S (IN)	TW (DEG R)	PE (LBF/FT2)	HE (BTU/LBM)	ME	Re_{x_T}	Re_θ	REDST
51	0.25	8.0	GRB	SP	0.95	2.140E 04	101.00	3.632E 03	4.384E 02	3.400E 02	11.77	4.290E 07	2.100E 03	4.750E 04
52	0.25	8.0	GRB	TFE	1.14	2.101E 04	101.00	1.799E 03	1.644E 02	2.740E 02	12.79	2.120E 07	1.840E 03	4.730E 04
53	0.50	9.0	GRB	GR	0.36	1.540E 04	47.60	2.404E 03	4.942E 03	1.938E 03	3.47	1.230E 07	1.600E 03	3.830E 03
54	0.86	9.0	GRW	CP	0.60	2.214E 04	62.50	3.988E 03	1.038E 03	2.603E 03	5.06	4.390E 06	1.020E 03	4.140E 03
55	0.63	9.0	GRW	CP	0.34	2.232E 04	65.50	2.876E 03	9.591E 02	1.268E 03	6.75	9.490E 06	1.570E 03	1.130E 04
56	0.63	9.0	GRW	CP	0.34	2.232E 04	65.50	2.876E 03	9.591E 02	1.268E 03	6.75	9.490E 06	1.570E 03	1.130E 04
57	0.50	8.6	TFE	SP	0.86	2.220E 04	41.98	3.299E 03	8.024E 02	1.567E 03	6.21	3.972E 06	1.006E 03	5.909E 03
58	0.50	8.6	TFE	CP	0.34	2.070E 04	40.64	2.665E 03	7.756E 02	1.452E 03	5.66	3.760E 06	8.904E 02	4.649E 03
59	0.25	8.0	TFE	TFE	1.28	2.160E 04	166.40	1.798E 03	9.251E 01	3.500E 02	11.85	1.464E 07	1.460E 03	2.914E 04
60	0.18	8.3	TFE	TFE	1.30	2.251E 04	133.30	1.799E 03	9.192E 01	3.760E 02	11.83	1.066E 07	1.196E 03	2.236E 04
61	0.25	8.0	TFE	TFE	1.26	2.248E 04	143.00	1.801E 03	1.103E 02	3.580E 02	12.09	1.500E 07	1.430E 03	2.860E 04
62	0.25	8.0	TFE	TFE	1.26	2.248E 04	143.00	1.801E 03	1.103E 02	3.580E 02	12.09	1.500E 07	1.430E 03	2.860E 04
63	0.50	8.0	TFE	CP	0.78	2.100E 04	40.40	3.392E 03	1.063E 03	1.760E 03	5.55	4.130E 06	9.410E 02	4.410E 03
64	0.25	8.0	TFE	TFE	1.26	2.263E 04	169.00	.799E 03	1.156E 02	3.570E 02	12.19	1.680E 07	1.840E 03	3.890E 04
65	0.25	8.0	TFE	TFE	1.21	2.260E 04	100.82	1.800E 03	1.367E 02	3.050E 02	13.15	1.667E 07	1.459E 03	3.556E 04
66	0.50	9.0	GRB	GR	0.50	1.935E 04	63.00	2.547E 03	4.369E 03	1.957E 03	4.71	2.000E 07	1.890E 03	6.630E 03
67	0.50	9.0	GRB	GR	0.25	1.005E 04	28.50	2.994E 03	3.679E 03	9.280E 02	2.84	9.180E 06	1.230E 03	3.970E 03
68	1.25	9.0	GRW	CP	0.90	2.269E 04	51.70	2.875E 03	7.792E 02	3.693E 03	4.12	1.540E 06	6.000E 02	1.650E 03
69	0.38	8.6	TFE	SP	0.63	2.130E 04	42.56	3.099E 03	6.472E 02	8.827E 02	7.52	8.754E 06	1.229E 03	1.074E 04
70	0.25	8.0	TFE	TFE	1.15	2.235E 04	101.00	1.800E 03	1.792E 02	3.040E 02	13.02	2.150E 07	1.720E 03	4.230E 04
71	0.50	9.0	TFE	CP	0.88	2.120E 04	65.90	2.471E 03	7.242E 02	7.160E 02	8.22	1.560E 07	1.460E 03	1.470E 04
72	0.38	8.6	TFE	SP	0.85	2.040E 04	42.10	3.395E 03	7.119E 02	7.922E 02	7.53	8.110E 06	1.185E 03	1.118E 04
73	0.25	22.0	GRB	BE	1.14	2.235E 04	31.80	1.030E 03	1.249E 03	1.685E 03	6.26	4.280E 06	7.340E 02	2.710E 03
74	0.25	22.0	GRB	BE	1.11	2.231E 04	24.30	1.309E 03	1.437E 03	1.680E 03	6.25	3.750E 06	6.860E 02	2.640E 03
75	0.25	22.0	GRB	BE	1.05	2.220E 04	14.60	1.614E 03	1.902E 03	1.587E 03	6.32	3.130E 06	6.220E 02	2.830E 03
76	0.25	8.0	TFE	TFE	1.23	2.263E 04	124.00	1.800E 03	1.265E 02	3.370E 02	12.51	1.650E 07	1.740E 03	3.930E 04
77	0.25	8.0	TFE	TFE	1.17	2.262E 04	78.40	1.800E 03	1.670E 02	3.050E 02	13.12	1.550E 07	1.710E 03	4.440E 04
78	0.25	8.0	TFE	TFE	1.09	2.258E 04	32.20	1.801E 03	2.420E 02	3.970E 02	11.50	6.390E 06	1.130E 03	2.270E 04
79	0.50	9.0	GRB	GR	0.33	1.460E 04	28.80	2.433E 03	4.987E 03	2.027E 03	3.06	6.430E 06	1.100E 03	2.310E 03
80	0.50	9.0	GRB	GR	0.31	1.406E 04	17.10	2.639E 03	3.978E 03	1.887E 03	3.03	3.210E 06	7.820E 02	1.580E 03
81	0.75	6.3	GRB	CP	0.73	2.198E 04	57.40	2.397E 03	6.817E 02	3.655E 03	4.05	1.630E 06	6.390E 02	1.550E 03
82	0.75	6.3	GRB	CP	0.72	2.195E 04	45.70	2.485E 03	6.319E 02	3.905E 03	3.60	1.040E 06	5.350E 02	1.080E 03
83	0.75	6.3	GRB	CP	0.67	2.179E 04	17.90	2.694E 03	7.575E 02	4.405E 03	3.44	3.750E 05	3.920E 02	4.340E 02
84	0.75	6.3	GRB	CP	0.59	2.143E 04	3.20	4.023E 03	3.210E 03	5.264E 03	2.81	1.870E 05	2.620E 02	7.730E 01
85	0.25	8.0	GRB	BE	1.18	2.177E 04	124.00	7.796E 02	1.491E 02	2.890E 02	12.94	2.270E 07	1.270E 03	2.750E 04
86	0.25	8.0	GRB	BE	0.98	2.146E 04	75.80	8.202E 02	3.745E 02	3.210E 02	12.13	2.970E 07	1.510E 03	2.980E 04
87	0.10	8.0	GRB	BE	1.18	2.259E 04	124.00	7.591E 02	1.600E 02	3.430E 02	12.38	2.000E 07	1.230E 03	2.320E 04
88	0.10	8.0	GRB	BE	1.07	2.253E 04	77.50	3.194E 02	2.693E 02	3.240E 02	12.70	2.260E 07	1.290E 03	2.630E 04
89	0.10	8.0	GRB	BE	0.94	2.245E 04	31.30	9.179E 02	4.866E 02	4.190E 02	11.22	1.150E 07	1.010E 03	1.700E 04
90	0.25	8.0	GRB	CP	0.87	2.058E 04	64.70	2.248E 03	5.772E 02	4.440E 02	9.97	2.370E 07	1.760E 03	2.800E 04
91	0.25	8.0	GRB	CP	0.83	2.048E 04	46.60	2.364E 03	6.888E 02	6.360E 02	8.45	1.200E 07	1.400E 03	1.620E 04
92	1.80	7.0	GRB	CP	0.65	2.159E 04	29.46	2.509E 03	1.031E 03	4.638E 03	3.24	7.513E 05	5.528E 02	5.191E 02
93	1.80	7.0	GRB	CP	0.65	2.159E 04	6.38	3.836E 03	2.601E 03	5.570E 03	2.73	2.836E 05	3.458E 02	1.520E 01
94	0.25	8.0	GRB	TFE	1.09	2.093E 04	56.50	1.800E 03	2.118E 02	3.310E 02	11.65	1.170E 07	1.480E 03	3.190E 04
95	0.25	8.0	GRB	TFE	0.92	2.062E 04	22.80	1.800E 03	4.712E 02	8.820E 02	7.37	2.500E 06	7.870E 02	6.710E 03
96	1.50	6.3	GRB	3DQP	0.75	2.253E 04	19.92	3.415E 03	5.173E 02	4.772E 03	3.48	5.453E 05	4.961E 02	7.633E 02
97	1.50	6.3	GRB	3DQP	0.72	2.243E 04	12.70	3.905E 03	1.032E 03	3.453E 03	3.09	2.710E 05	3.640E 02	2.210E 02
98	0.50	9.0	GRB	GR	0.38	1.680E 04	8.20	2.804E 03	3.681E 03	2.749E 03	3.13	1.150E 06	5.410E 02	8.830E 02
99	2.04	5.9	GRB	3DQP	0.89	2.288E 04	46.40	2.337E 03	2.649E 02	5.046E 03	3.49	3.180E 05	3.740E 02	4.290E 02
100	2.04	5.9	GRB	3DQP	0.35	2.272E 04	33.30	2.536E 03	3.687E 02	5.177E 03	3.36	2.970E 05	3.750E 02	3.640E 02

TABLE 2. LOCAL TRANSITION PROPERTIES (CONT.)

DATA POINT	RN (IN)	θc (DEG)	NOSE MAT.	FRUST. MAT.	HBAR	U(INF) (FT/SEC)	S (IN)	TW (DEG R)	PE (LBF/FT2)	HE (BTU/LBM)	ME	Re xT	Re θ	REDST
101	2.04	5.9	GRB	3DQP	0.78	2.240E 04	12.30	3.642E 03	9.315E 02	5.671E 03	2.99	2.230E 05	3.458E 02	1.336E 02
102	0.25	8.6	GRB	SP	0.66	2.077E 04	23.60	4.602E 03	1.893E 03	3.279E 03	4.02	1.990E 06	7.090E 02	2.290E 03
103	0.25	8.6	GRB	SP	0.64	2.067E 04	18.20	4.991E 03	1.854E 03	3.589E 03	3.66	1.260E 06	6.580E 02	2.050E 03
104	1.50	8.6	GRB	SP	0.64	1.965E 04	20.40	4.993E 03	1.256E 03	3.896E 03	3.12	7.430E 05	4.870E 02	7.240E 02
105	1.50	8.6	GRB	SP	0.64	1.965E 04	13.20	5.000E 03	1.461E 03	4.018E 03	3.02	5.155E 05	4.325E 02	4.698E 02
106	0.50	9.0	GRB	GR	0.33	1.258E 04	28.30	2.651E 03	3.820E 03	1.442E 03	3.00	6.230E 06	1.100E 03	2.800E 03
107	0.50	9.0	GRB	GR	0.29	1.148E 04	16.60	2.946E 03	3.020E 03	1.196E 03	2.93	3.390E 06	7.730E 02	2.250E 03
108	0.25	22.0	GRB	BE	1.15	2.236E 04	31.80	1.013E 03	1.192E 03	1.667E 03	6.27	4.090E 06	7.160E 02	2.610E 03
109	0.25	22.0	GRB	BE	1.13	2.232E 04	24.40	1.100E 03	1.342E 03	1.682E 03	6.26	3.510E 06	6.710E 02	2.600E 03
110	0.25	22.0	GRB	BE	1.08	2.224E 04	14.60	1.324E 03	1.652E 03	1.628E 03	6.29	2.660E 06	5.860E 02	2.420E 03
111	0.25	22.0	GRB	BE	1.16	2.237E 04	31.80	1.014E 03	1.165E 03	1.688E 03	6.27	4.000E 06	7.070E 02	2.570E 03
112	0.25	22.0	GRB	BE	1.11	2.230E 04	24.30	1.232E 03	1.435E 03	1.678E 03	6.25	3.760E 06	6.840E 02	2.570E 03
113	0.25	22.0	GRB	BE	1.06	2.205E 04	14.60	1.577E 03	1.789E 03	1.586E 03	6.28	2.940E 06	6.140E 02	2.630E 03
114	0.10	8.0	GRB	SP	1.17	2.258E 04	167.00	2.036E 03	1.065E 02	3.510E 02	12.24	2.720E 07	1.620E 03	3.250E 04
115	0.10	8.0	GRB	SP	1.09	2.255E 04	120.40	2.273E 03	2.449E 02	3.460E 02	12.26	2.898E 07	1.658E 03	3.434E 04
116	0.10	8.0	GRB	SP	1.07	2.253E 04	122.00	2.297E 03	2.693E 02	3.170E 02	12.63	3.660E 07	1.930E 03	4.470E 04
117	0.10	8.0	GRB	SP	1.00	2.247E 04	77.00	2.613E 03	3.732E 02	3.410E 02	12.36	2.900E 07	1.750E 03	3.850E 04
118	0.10	8.0	GRB	SP	1.00	2.247E 04	72.08	2.653E 03	3.732E 02	3.379E 02	12.42	2.747E 07	1.699E 03	3.815E 04
119	0.10	8.0	GRB	SP	0.97	2.245E 04	33.40	3.310E 03	4.268E 02	2.994E 02	13.13	1.721E 07	1.253E 03	3.335E 04
120	0.10	8.0	GRB	SP	0.97	2.245E 04	12.60	1.955E 03	4.240E 02	4.404E 02	10.92	3.790E 06	6.084E 02	1.015E 04
121	0.25	8.0	TFE	TFE	1.23	2.262E 04	124.00	1.800E 03	1.301E 02	3.550E 02	12.22	1.550E 07	1.690E 03	3.600E 04
122	0.20	8.0	TFE	TFE	1.19	2.262E 04	78.40	1.801E 03	1.530E 02	3.140E 02	12.94	1.370E 07	1.600E 03	3.970E 04
123	0.25	8.0	TFE	TFE	1.05	2.256E 04	33.40	1.799E 03	2.929E 02	3.380E 02	12.47	1.000E 07	1.370E 03	3.240E 04
124	0.64	5.9	GRB	QP	0.40	1.668E 04	34.82	3.453E 03	1.582E 03	2.383E 03	3.53	2.639E 06	7.822E 02	1.790E 03
125	0.64	5.9	GRB	QP	0.34	1.577E 04	16.50	3.863E 03	2.160E 03	2.184E 03	3.59	1.710E 06	6.870E 02	1.410E 03
126	0.64	5.9	GRB	QP	0.43	1.480E 04	41.60	2.783E 03	1.216E 03	1.788E 03	3.46	2.920E 06	7.880E 02	1.920E 03
127	0.64	5.9	GRB	QP	0.27	1.307E 04	20.50	3.088E 03	2.124E 03	1.553E 03	3.32	2.620E 06	7.920E 02	1.770E 03
128	1.20	5.9	GRB	QP	0.54	1.496E 04	38.10	2.091E 03	6.741E 02	1.870E 03	3.46	1.450E 06	6.180E 02	1.230E 03
129	1.20	5.9	GRB	QP	0.38	1.400E 04	16.30	2.949E 03	1.700E 03	1.738E 03	3.22	1.540E 06	6.810E 02	1.300E 03
130	1.80	7.0	GRB	CP	0.66	2.169E 04	29.46	2.492E 03	9.954E 02	4.703E 03	3.24	7.132E 05	5.395E 02	5.026E 02
131	1.80	7.0	GRB	CP	0.64	2.145E 04	14.30	2.894E 03	1.601E 03	4.961E 03	3.01	4.900E 05	4.680E 02	2.200E 02
132	1.80	7.0	GRB	CP	0.64	2.145E 04	6.50	3.912E 03	2.753E 03	5.402E 03	2.74	3.177E 05	3.643E 02	1.203E 01
133	0.25	8.0	GRB	SP	0.87	2.252E 04	56.40	3.266E 03	6.802E 02	8.430E 02	8.27	1.050E 07	1.410E 03	1.500E 04
134	0.25	8.0	GRB	BE	0.91	2.267E 04	60.00	8.790E 02	5.730E 02	4.060E 02	11.49	2.740E 07	1.540E 03	2.620E 04
135	0.25	8.0	GRB	BE	0.72	2.220E 04	22.60	1.215E 03	1.400E 03	1.734E 03	6.14	3.280E 06	7.370E 02	3.430E 03
136	0.25	8.0	GRB	SP	0.83	2.337E 04	22.80	3.236E 03	9.286E 02	1.448E 03	6.96	2.870E 06	7.190E 02	4.880E 03
137	0.25	8.0	TFE	TFE	1.12	2.274E 04	56.00	1.801E 03	2.168E 02	3.760E 02	11.94	1.080E 07	1.530E 03	3.350E 04
138	0.25	8.0	TFE	TFE	0.99	2.270E 04	22.20	1.801E 03	4.148E 02	9.540E 02	7.93	2.130E 06	8.110E 02	7.750E 03
139	0.25	8.0	TFE	TFE	1.08	2.212E 04	56.00	1.799E 03	2.466E 02	3.730E 02	11.65	1.220E 07	1.610E 03	3.430E 04
140	0.25	8.0	TFE	TFE	0.99	2.209E 04	22.20	1.801E 03	3.954E 02	9.010E 02	7.88	2.140E 06	9.470E 02	1.120E 04
141	0.25	8.0	GRB	SP	0.86	2.113E 04	56.40	3.497E 03	6.478E 02	7.090E 02	8.32	1.210E 07	1.380E 03	1.570E 04
142	0.25	8.0	GRB	SP	0.83	2.104E 04	22.80	3.961E 03	7.315E 02	3.193E 03	4.23	8.200E 05	4.450E 02	1.540E 03
143	0.86	9.0	GRW	CP	0.61	2.125E 04	18.30	4.505E 03	1.769E 03	4.325E 03	3.34	8.600E 05	4.960E 02	8.800E 02
144	0.25	10.0	GRB	CP	0.74	2.160E 04	23.08	1.329E 03	1.773E 03	1.562E 03	5.96	5.300E 06	1.009E 03	4.210E 03
145	1.50	6.3	GRB	3DQP	0.75	2.253E 04	51.44	2.734E 03	4.947E 02	4.637E 03	3.60	6.790E 05	5.705E 02	9.270E 02
146	0.50	9.0	GRB	GR	0.45	1.650E 04	15.20	2.570E 03	3.392E 03	3.324E 03	3.24	1.760E 06	5.950E 02	9.510E 02
147	0.50	9.0	GRB	GR	0.48	1.905E 04	33.50	2.515E 03	4.943E 03	3.353E 03	3.38	5.750E 06	9.830E 02	1.840E 03
148	1.25	9.0	GRW	CP	0.53	2.105E 04	8.85	3.232E 03	3.175E 03	4.745E 03	3.00	5.990E 05	5.000E 02	3.120E 02
149	0.86	9.0	GRW	CP	0.75	2.199E 04	48.70	4.204E 03	1.541E 03	3.511E 03	4.23	3.270E 06	8.200E 02	2.730E 03

REENTRY F

TRANSITION RESULTS

FROM REF. 13

TABLE I.- TEST CONDITIONS AT BEGINNING OF TRANSI[illegible]N

h		r		x		$R_{e,x}$	M_e	$\frac{H_w}{H_e}$	δ^*		θ	
km	ft	cm	in.	m	ft				cm	in.	cm	in.
Small nose radius												
30.480	100 000	0.3149	0.124	2.926	9.6	43.5×10^6	15.11	1.01	3.111×10^{-2}	1.225×10^{-2}	9.957×10^{-4}	3.92×10^{-4}
29.870	98 000	.3200	.126	2.835	9.3	46.0	15.09	1.00	2.896	1.14	9.271	3.65
29.261	96 000	.3226	.127	2.743	9.0	48.5	15.05	.99	2.718	1.07	8.636	3.40
28.651	94 000	.3277	.129	2.438	8.0	47.0	14.99	.98	2.535	.998	8.052	3.17
28.042	92 000	.3302	.130	2.377	7.8	49.5	14.95	.98	2.375	.935	7.544	2.97
27.432	90 000	.3353	.132	2.316	7.6	54.0	14.91	.97	2.230	.878	7.036	2.77
26.822	88 000	.3391	.1335	2.256	7.4	56.5	14.83	.98	2.121	.835	6.655	2.62
26.213	86 000	.3429	.135	2.225	7.3	60.5	14.74	.98	1.999	.787	6.350	2.50
25.908	85 000	.3467	.1365	2.195	7.2	62.0	14.74	.98	1.943	.765	6.172	2.43
25.603	84 000	.3480	.137	2.164	7.1	63.0	14.62	.98	1.877	.739	6.045	2.38
24.994	82 000	.3531	.139	2.073	6.8	64.0	14.52	.98	1.753	.690	5.715	2.25
24.384	8[illegible] 000	.3581	.141	2.012	6.6	68.0	14.43	.98	1.626	.640	5.461	2.15
23.774	78 000	.3632	.143	1.676	5.5	58.0	13.99	1.00	1.440	.567	5.080	2.00
23.165	76 000	.3683	.145	1.615	5.3	57.0	13.75	1.01	1.260	.496	4.801	1.89
22.860	75 000	.3721	.1465	1.433	4.7	49.0	13.41	1.02	1.176	.463	4.623	1.82
22.555	74 000	.3747	.1475	1.402	4.6	47.0	13.23	1.04	1.118	.440	4.521	1.78
21.946	72 000	.3810	.150	1.341	4.4	47.5	12.94	1.09	1.008	.397	4.394	1.73
21.336	70 000	.3861	.152	1.219	4.0	41.5	12.40	1.13	.904	.356	4.318	1.70
20.726	68 000	.3937	.155	.930	3.05	22.5	11.00	1.20	.777	.306	4.318	1.70
20.117	66 000	.3988	.157	.872	2.86	19.5	10.40	1.40	.650	.256	4.394	1.73
19 812	65 000	.4013	.158	.853	2.8	19.0	10.20	1.54	.584	.230	4.496	1.77
19.507	64 000	.4064	.160	.808	2.65	16.5	9.70	1.84	.513	.202	4.902	1.93
18.898	62 000	.4140	.163	.686	2.25	10.5	8.75	2.65	.386	.152	5.944	2.34
18.288	60 000	.4204	.1655	.427	1.40	2.2	6.17	3.80	.277	.109	7.569	2.98
Large nose radius												
30.480	100 000	0.3150	0.124	2.926	9.6	43.5×10^6	15.11	1.01	3.111×10^{-2}	1.225×10^{-2}	9.957×10^{-4}	3.92×10^{-4}
29.870	98 000	.3200	.126	2.835	9.3	46.5	15.09	1.00	2.921	1.15	9.322	3.67
29.261	96 000	.3277	.129	2.743	9.0	46.5	15.02	1.00	2.743	1.08	8.738	3.44
28.651	94 000	.3404	.134	2.438	8.0	46.0	14.90	1.00	2.548	1.003	8.230	3.24
28.042	92 000	.3569	.1405	2.377	7.8	48.0	14.80	1.00	2.433	.958	7.747	3.05
27.432	90 000	.3734	.147	2.316	7.6	51.0	14.70	1.00	2.250	.886	7.239	2.85
26.882	88 000	.3886	.153	2.256	7.4	54.0	14.52	1.01	2.113	.832	6.858	2.70
26.213	86 000	.4089	.161	2.225	7.3	56.0	14.37	1.015	1.976	.778	6.604	2.60
25.908	85 000	.4178	.1645	2.195	7.2	57.4	14.29	1.02	1.892	.745	6.477	2.55
25.603	84 000	.4280	.1685	2.164	7.1	57.0	14.13	1.03	1.849	.728	6.299	2.48
24.994	82 000	.4496	.177	2.073	6.8	57.0	13.85	1.05	1.715	.675	6.096	2.40
24.384	80 000	.4775	.188	2.012	6.6	57.0	13.6	1.08	1.588	.625	6.045	2.38
23.774	78 000	.5080	.200	1.676	5.5	39.5	12.53	1.22	1.372	.540	6.147	2.42
23.165	76 000	.5436	.214	1.615	5.3	34.0	11.83	1.45	1.130	.445	6.477	2.55
22.860	75 000	.5613	.221	1.433	4.7	24.5	11.04	1.575	1.019	.401	6.731	2.65
22.555	74 000	.5817	.229	1.402	4.6	22.0	10.58	1.75	.953	.375	7.010	2.76
21.946	72 000	.6172	.243	1.341	4.4	17.2	9.6	2.08	.826	.325	7.874	3.10
21.336	70 000	.6731	.265	1.219	4.0	11.0	8.4	2.60	.706	.278	8.992	3.54
20.726	68 000	.7290	.287	.930	3.05	3.85	6.5	3.65	.577	.227	11.430	4.50
20.117	66 000	.7874	.310	.872	2.86	2.6	5.75	5.1	.465	.183	14.732	5.80
19.812	65 000	.8179	.322	.853	2.8	2.33	5.5	5.96	.422	.166	16.129	6.35
19.507	64 000	.8687	.342	.808	2.65	1.90	5.22	6.68	.399	.157	17.399	6.85
18.898	62 000	.9169	.361	.686	2.25	1.25	4.70	8.25	.361	.142	19.126	7.53
18.288	60 000	.9881	.389	.427	1.40	.61	4.15	9.85	.3366	.1325	20.650	8.13

TABLE II.- TEST CONDITIONS AT END OF TRANSITION

h		r		x		$R_{e,x}$	M_e	$\frac{H_w}{H_e}$	δ^*		θ	
km	ft	cm	in.	m	ft				cm	in.	cm	in.
Small nose radius												
25.603	84 000	0.3480	0.137	3.353	11.0	98×10^6	14.69	0.695	7.137×10^{-2}	2.81×10^{-2}	22.860×10^{-4}	9.0×10^{-4}
24.994	82 000	.3531	.139	3.231	10.6	105	14.7	.71	7.163	2.82	22.301	8.78
24.384	80 000	.3581	.141	3.139	10.3	111	14.7	.74	7.188	2.83	22.962	9.04
23.774	78 000	.3632	.143	2.957	9.7	116	14.74	.75	6.502	2.56	21.082	8.3
23.165	76 000	.3683	.145	2.835	9.3	124	14.75	.73	6.058	2.385	19.812	7.8
22.860	75 000	.3721	.1465	2.652	8.7	125	14.91	.72	5.410	2.13	17.780	7.0
22.555	74 000	.3747	.1475	2.560	8.4	132	15.00	.70	5.144	2.025	16.942	6.67
21.946	72 000	.3810	.150	2.499	8.2	142	15.00	.665	5.144	2.025	17.577	6.92
21.336	70 000	.3861	.152	2.408	7.9	150	14.97	.625	5.156	2.03	17.374	6.84
20.726	68 000	.3937	.155	2.316	7.6	162	15.01	.595	5.207	2.05	16.688	6.57
20.117	66 000	.3988	.157	2.286	7.5	178	15.00	.565	5.512	2.17	16.485	6.49
19.812	65 000	.4013	.158	2.286	7.5	188	15.01	.55	5.639	2.22	16.447	6.475
19.507	64 000	.4064	.160	2.286	7.5	198	15.05	.53	5.817	2.29	16.383	6.45
18.898	62 000	.4140	.163	2.285	7.5	218	15.10	.50	6.121	2.41	16.180	6.37
18.288	60 000	.4204	.1655	2.286	7.5	241	15.15	.46	6.401	2.52	15.939	6.275
Large nose radius												
25.603	84 000	0.4280	0.1685	3.353	11.0	107×10^6	14.98	0.71	6.883×10^{-2}	2.71×10^{-2}	21.234×10^{-4}	8.36×10^{-4}
24.994	82 000	.4496	.177	3.231	10.6	115	15.11	.70	6.071	2.39	18.644	7.34
24.384	80 000	.4775	.188	3.139	10.3	125	15.17	.71	5.436	2.14	16.510	6.50
23.774	78 000	.5080	.200	2.957	9.7	128	15.16	.71	5.207	2.05	17.399	6.85
23.165	76 000	.5436	.214	2.835	9.3	132	15.12	.70	5.652	2.225	21.844	8.60
22.860	75 000	.5613	.221	2.652	8.7	130	15.08	.70	5.512	2.17	22.200	8.74
22.555	74 000	.5817	.229	2.560	8.4	128	14.98	.70	5.029	1.98	19.685	7.75
21.946	72 000	.6172	.243	2.499	8.2	134	14.81	.675	4.343	1.71	16.066	6.325
21.336	70 000	.6731	.265	2.408	7.9	141	14.70	.65	3.835	1.51	13.208	5.20
20.726	68 000	.7290	.287	2.316	7.6	149	14.69	.625	4.115	1.62	14.732	5.80
20.117	66 000	.7874	.310	2.286	7.5	165	14.70	.58	5.436	2.14	17.209	6.775
19.812	65 000	.8179	.322	2.286	7.5	175	14.77	.55	6.121	2.41	18.415	7.25
19.507	64 000	.8687	.342	2.286	7.5	185	14.78	.54	6.401	2.52	18.567	7.31
18.898	62 000	.9169	.361	2.286	7.5	209	14.79	.50	6.883	2.71	18.720	7.37
18.288	60 000	.9881	.389	2.286	7.5	233	14.80	.49	7.290	2.87	16.840	6.63

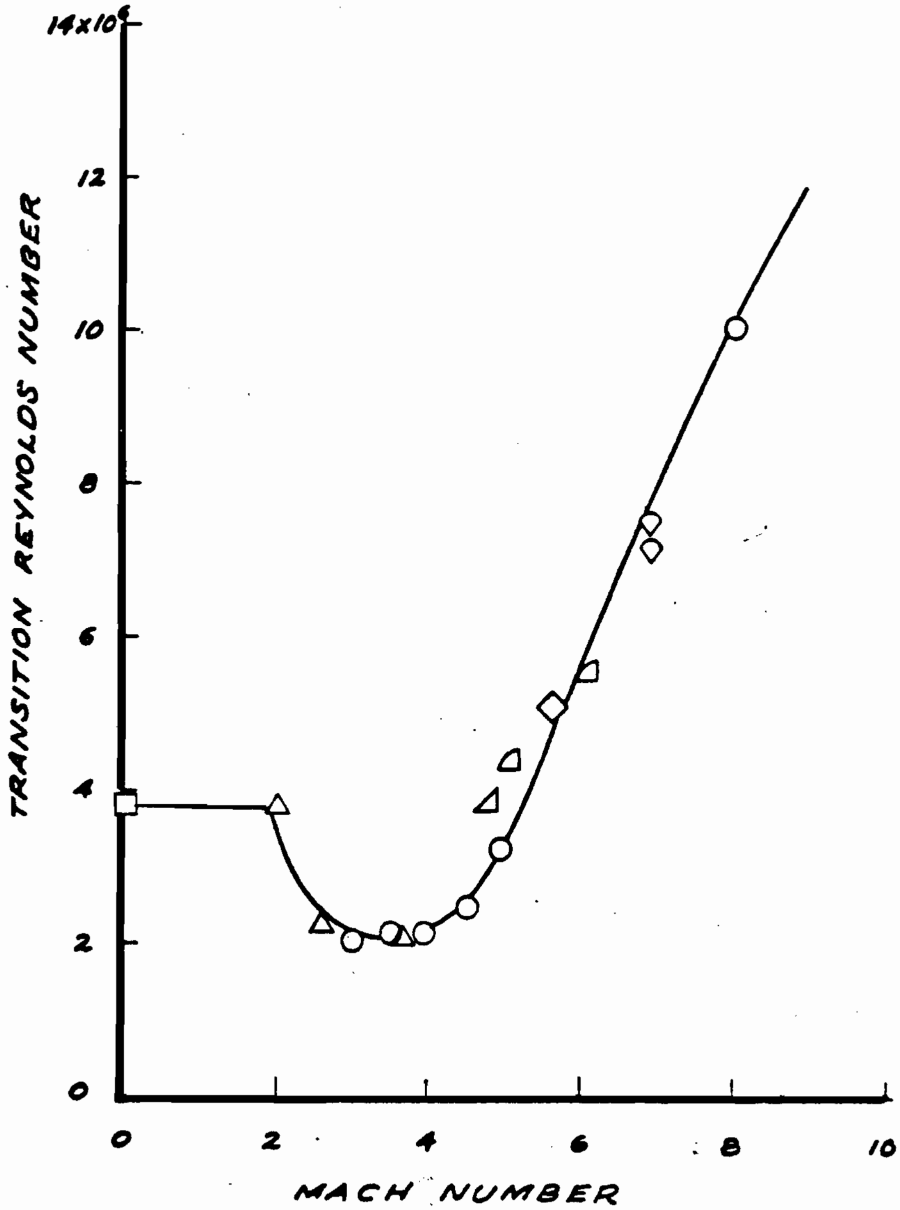

FIG. 1. Effect of Mach Number on Transition

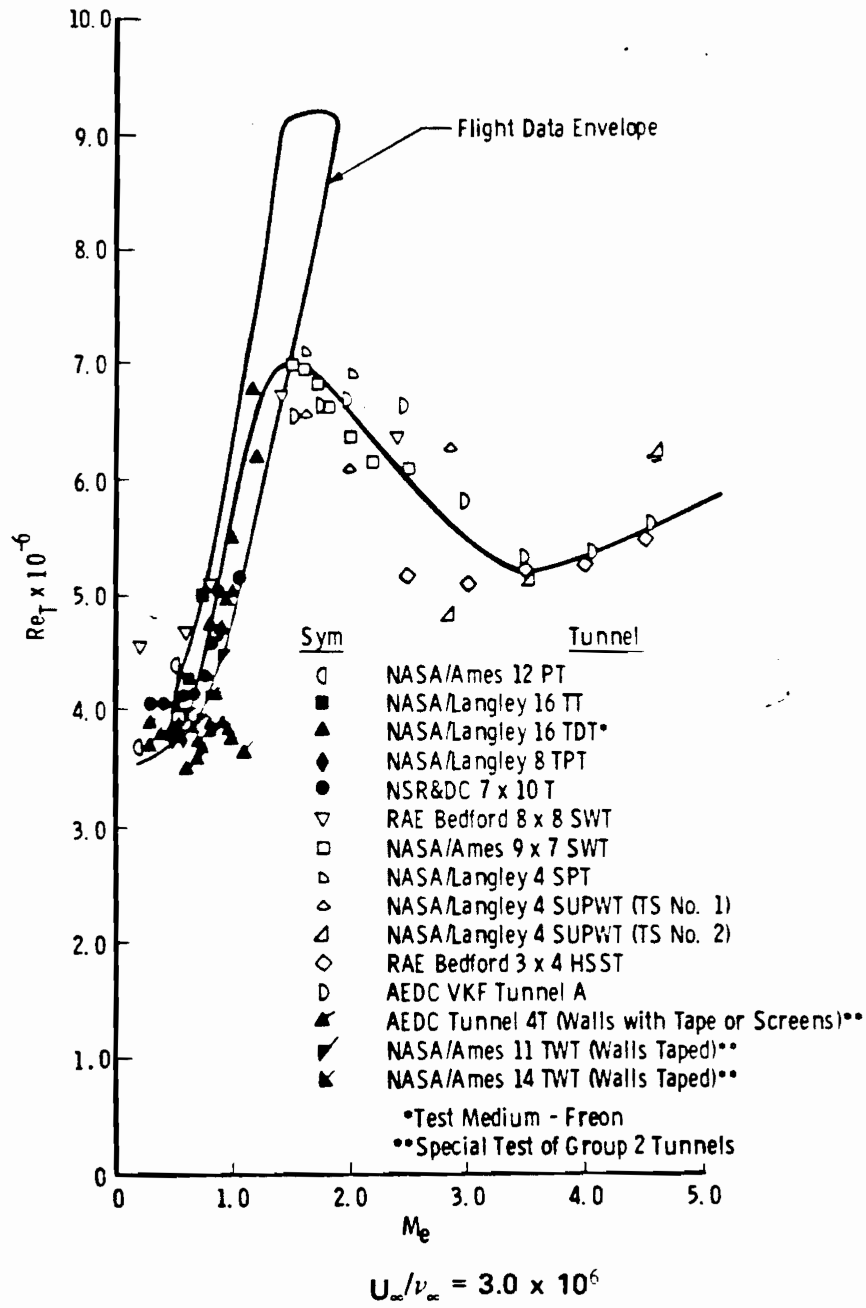

FIG. 2. Wind Tunnel and Flight Transition Results

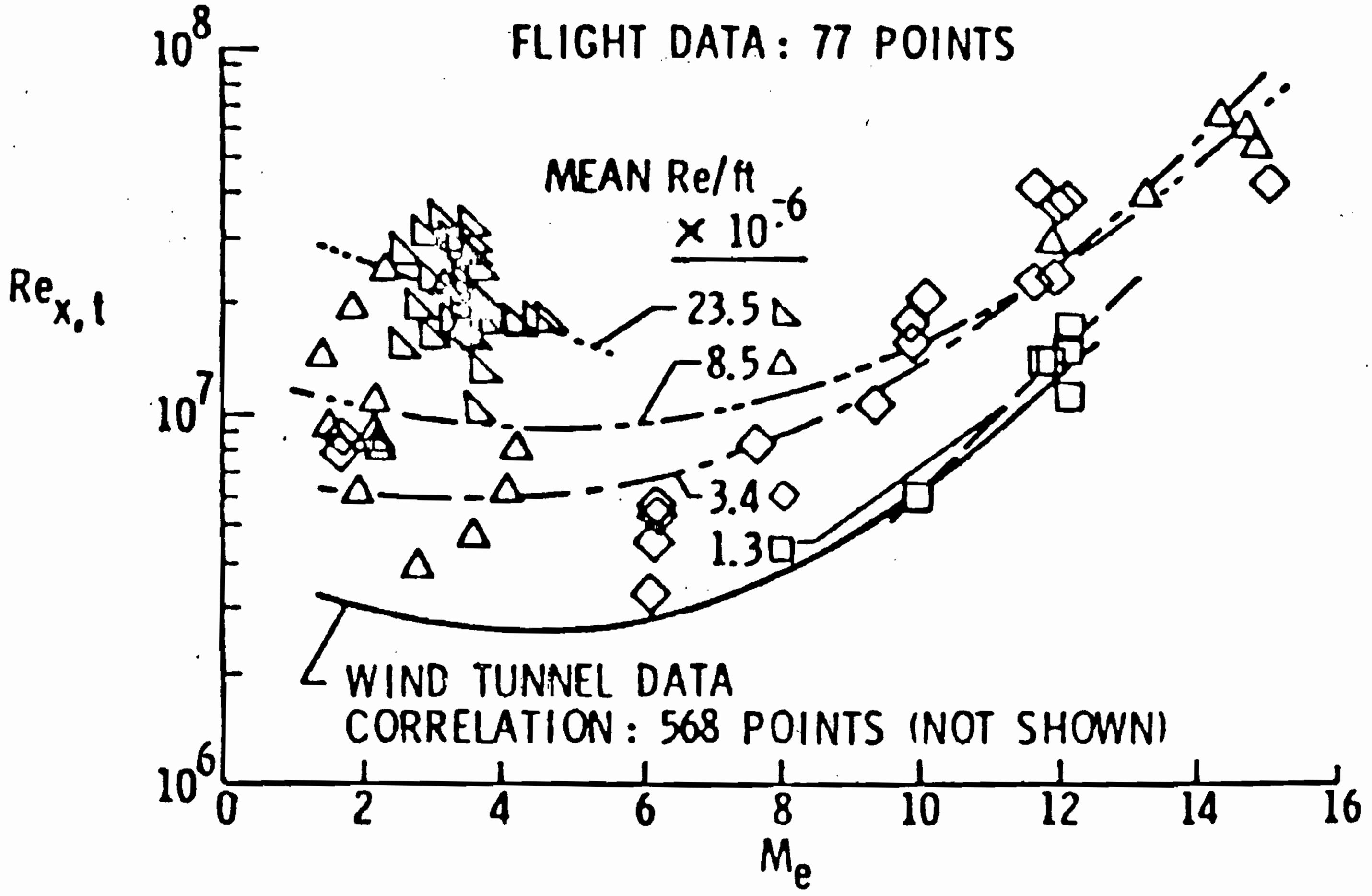

FIG. 3. Transition Reynolds Number Data
on
Sharp Cones in Wind Tunnels and in Flight

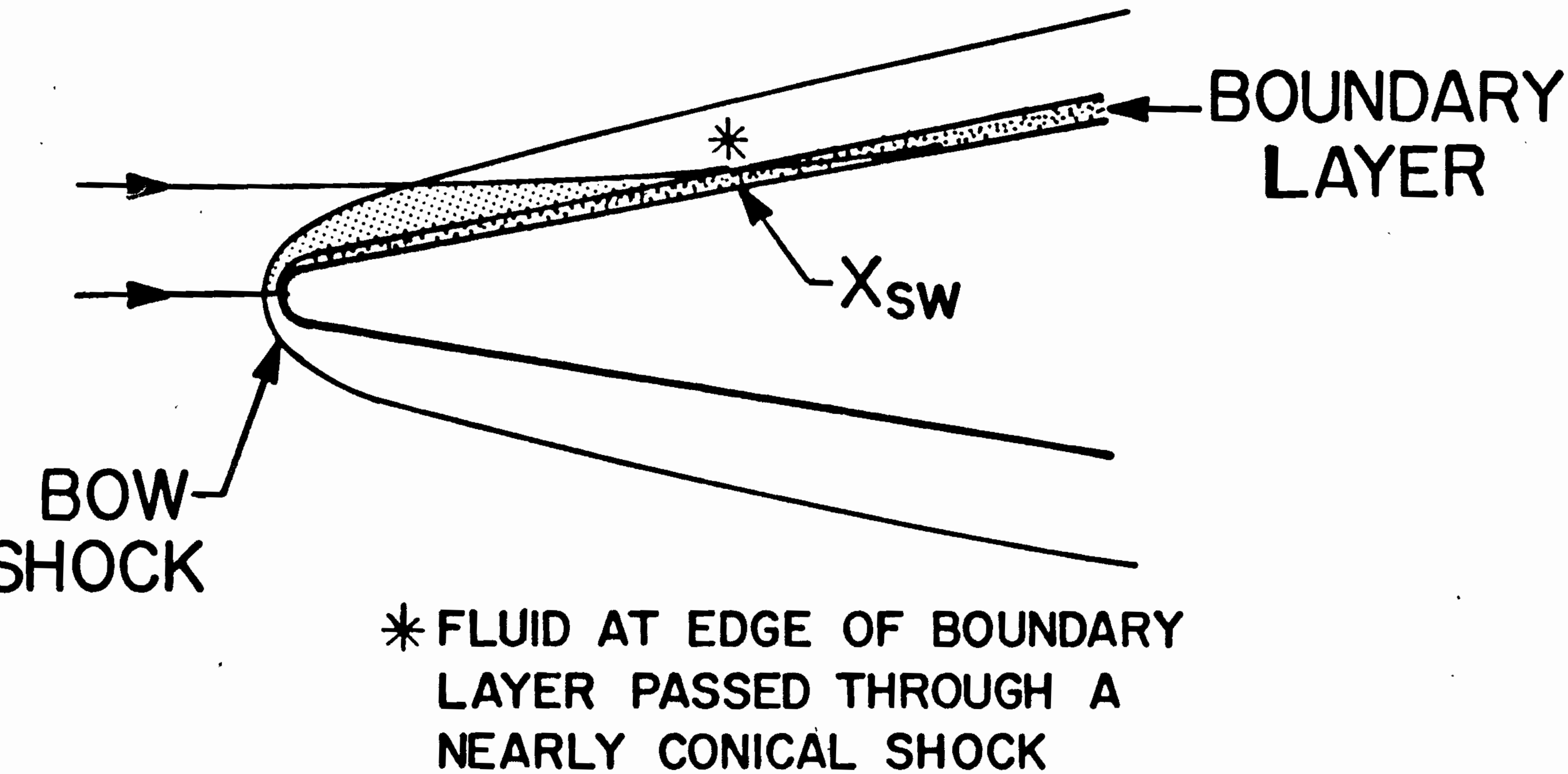

FIG. 4 A Schematic of Flow Over a Slender Blunt Cone

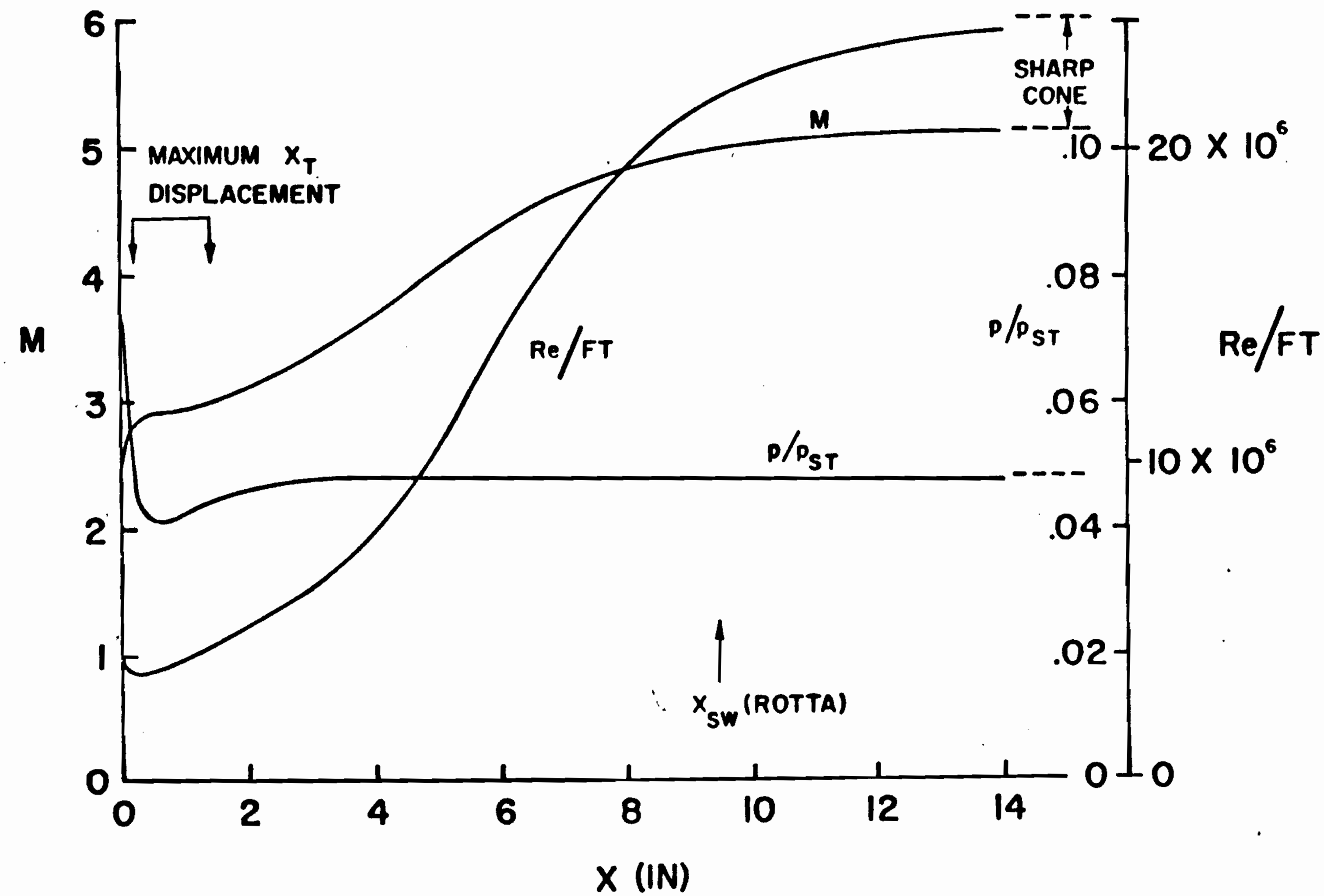

FIG. 5. Calculations of Local Flow Properties on an 8-Degree Half Angle Cone With 2% Bluntness at M_∞ = 5.9

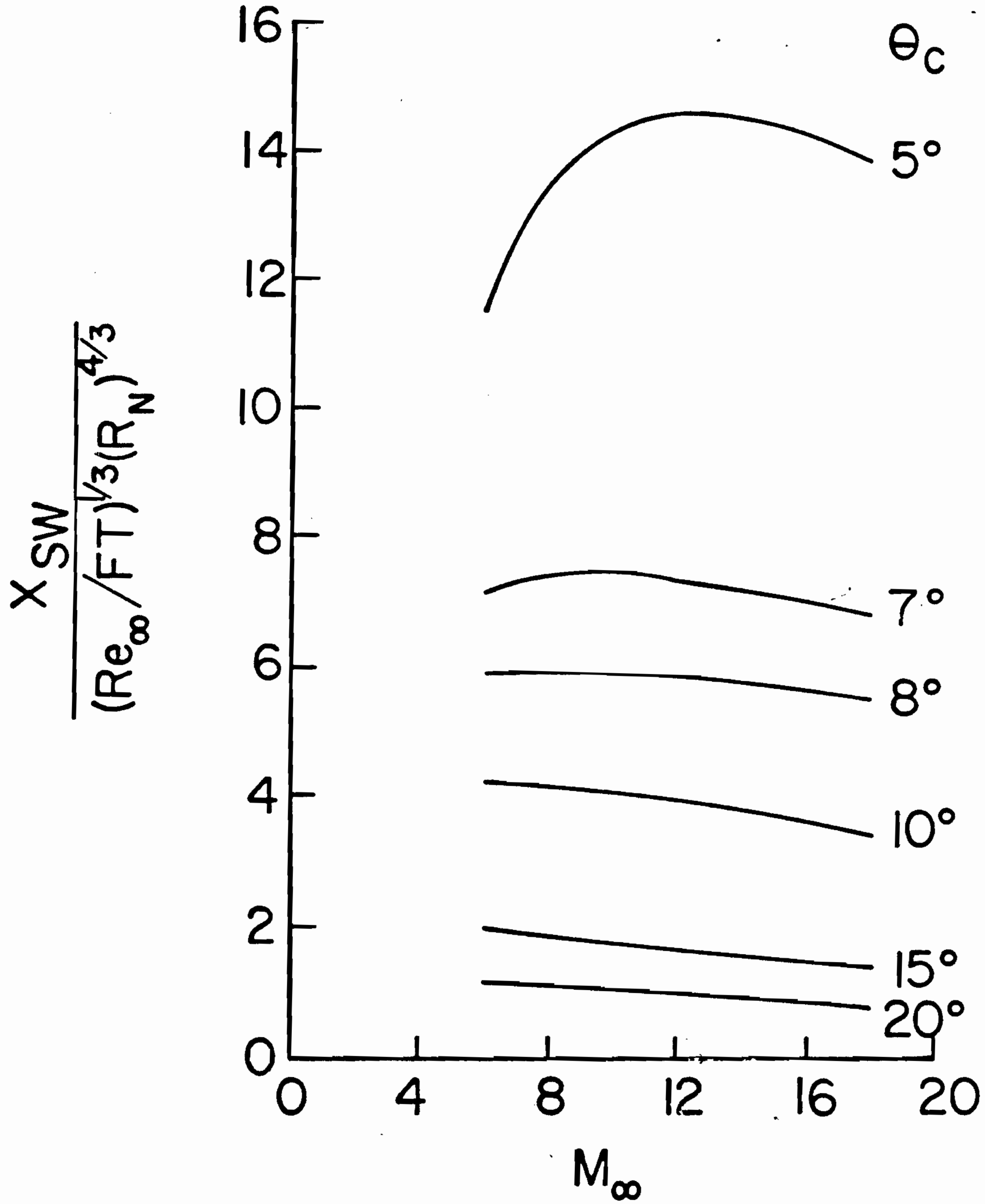

FIG. 6. Entropy-Layer-Swallowing Distance Parameter

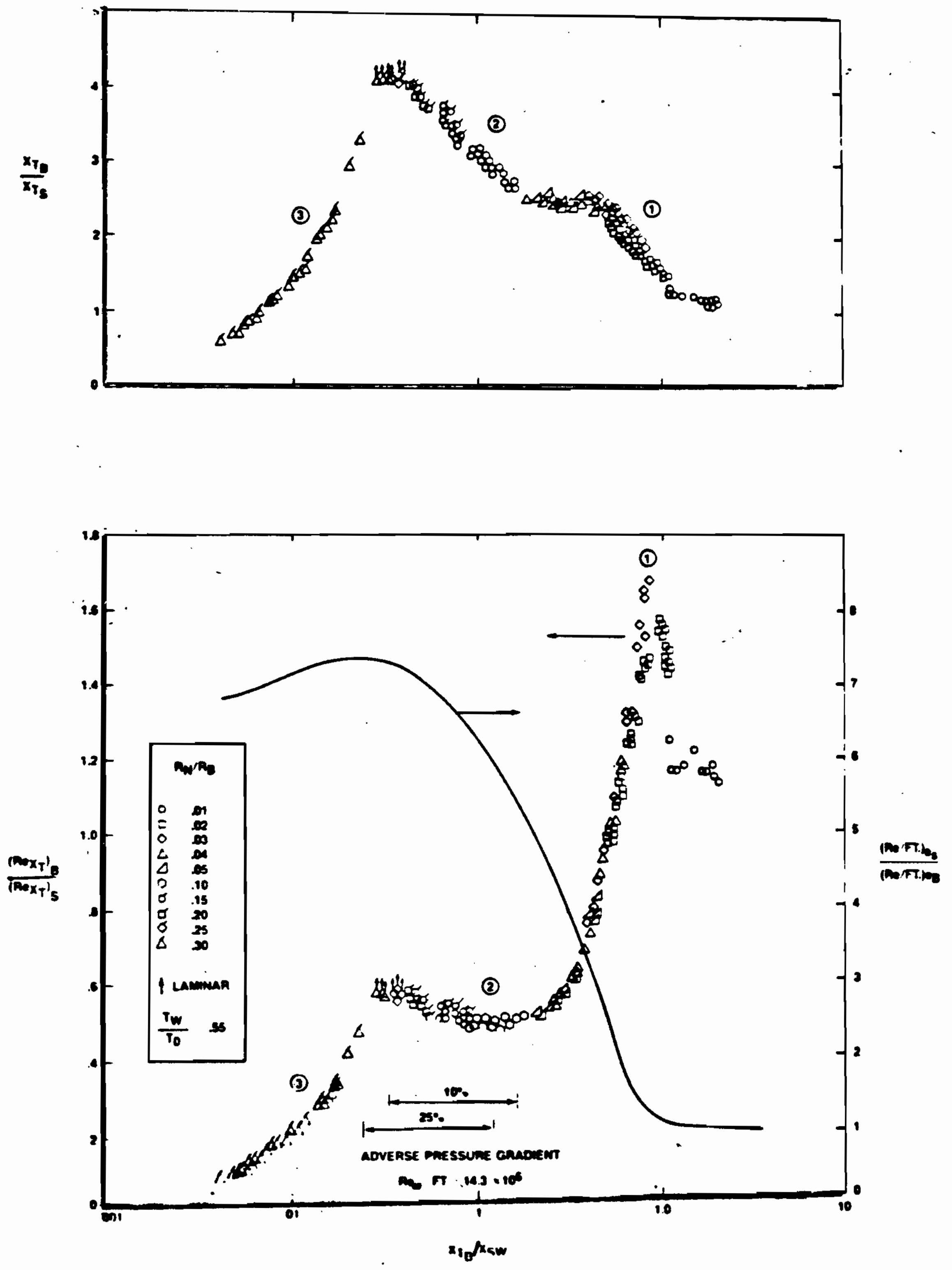

FIG. 7. Effect of Nosetip Bluntness on Cone Frustum Transition at $M_\infty = 5.9$

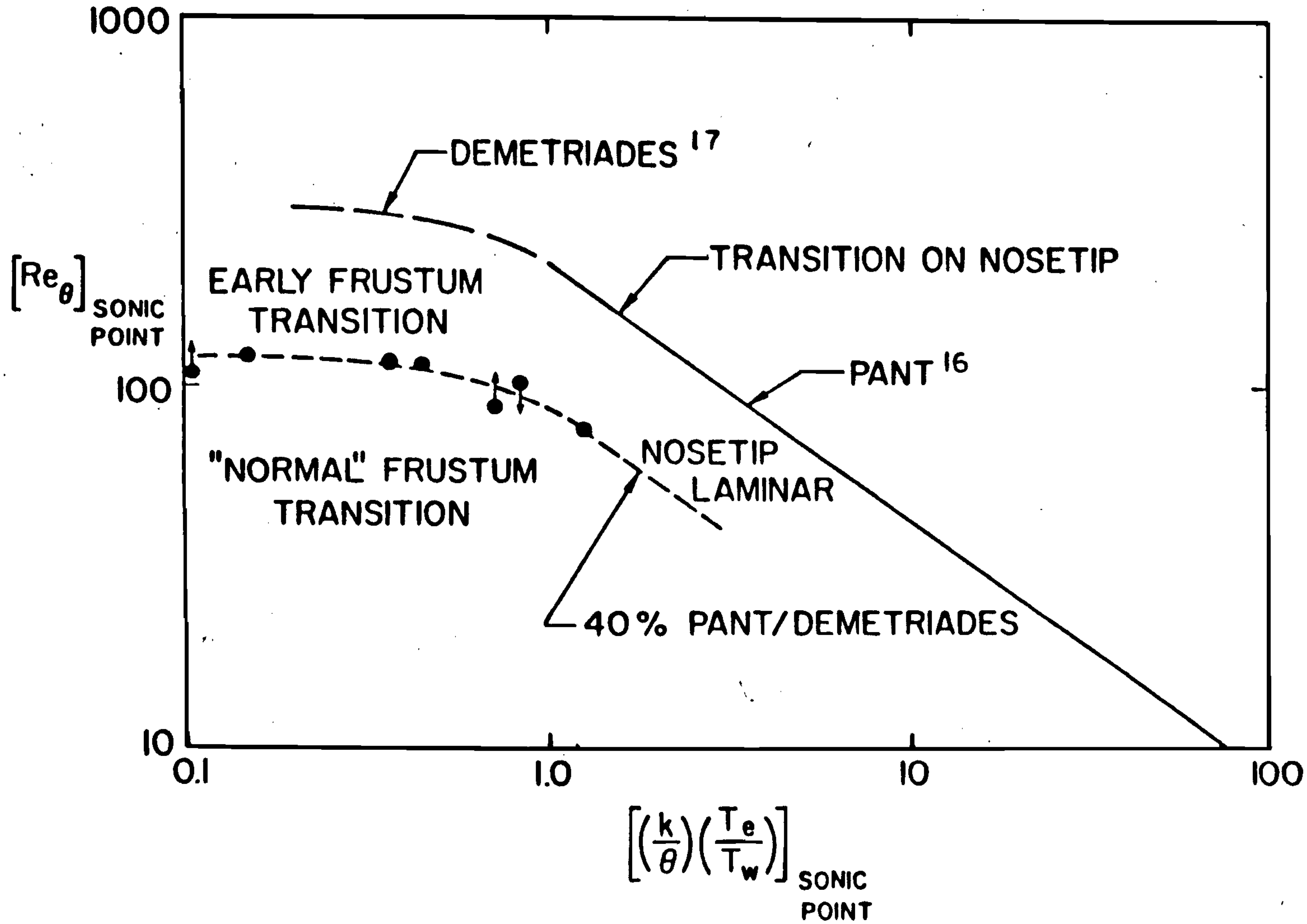

FIG. 8. Nosetip Instability Effects on Cone Frustum Transition

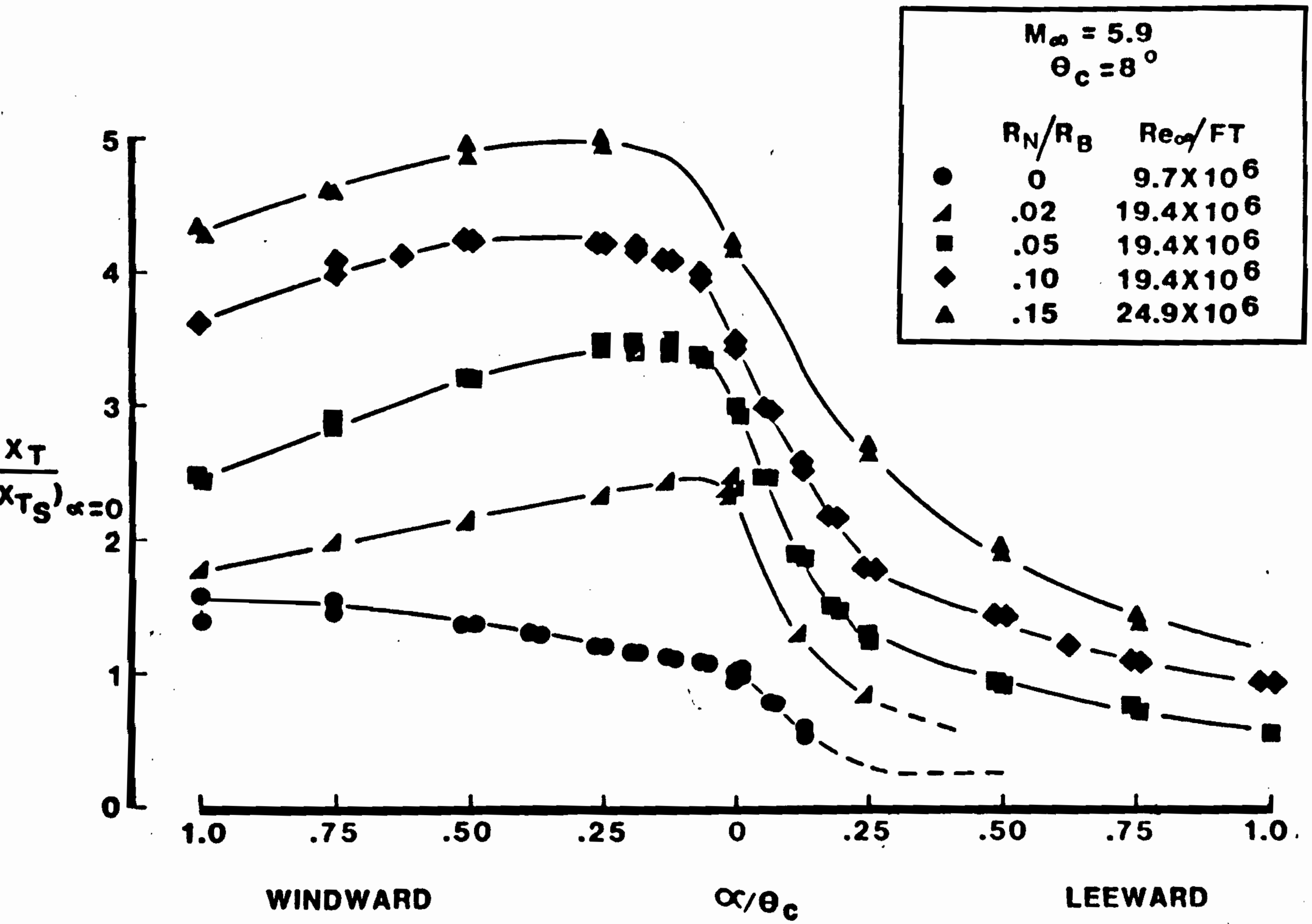

FIG. 9. Transition Movement With Angle of Attack

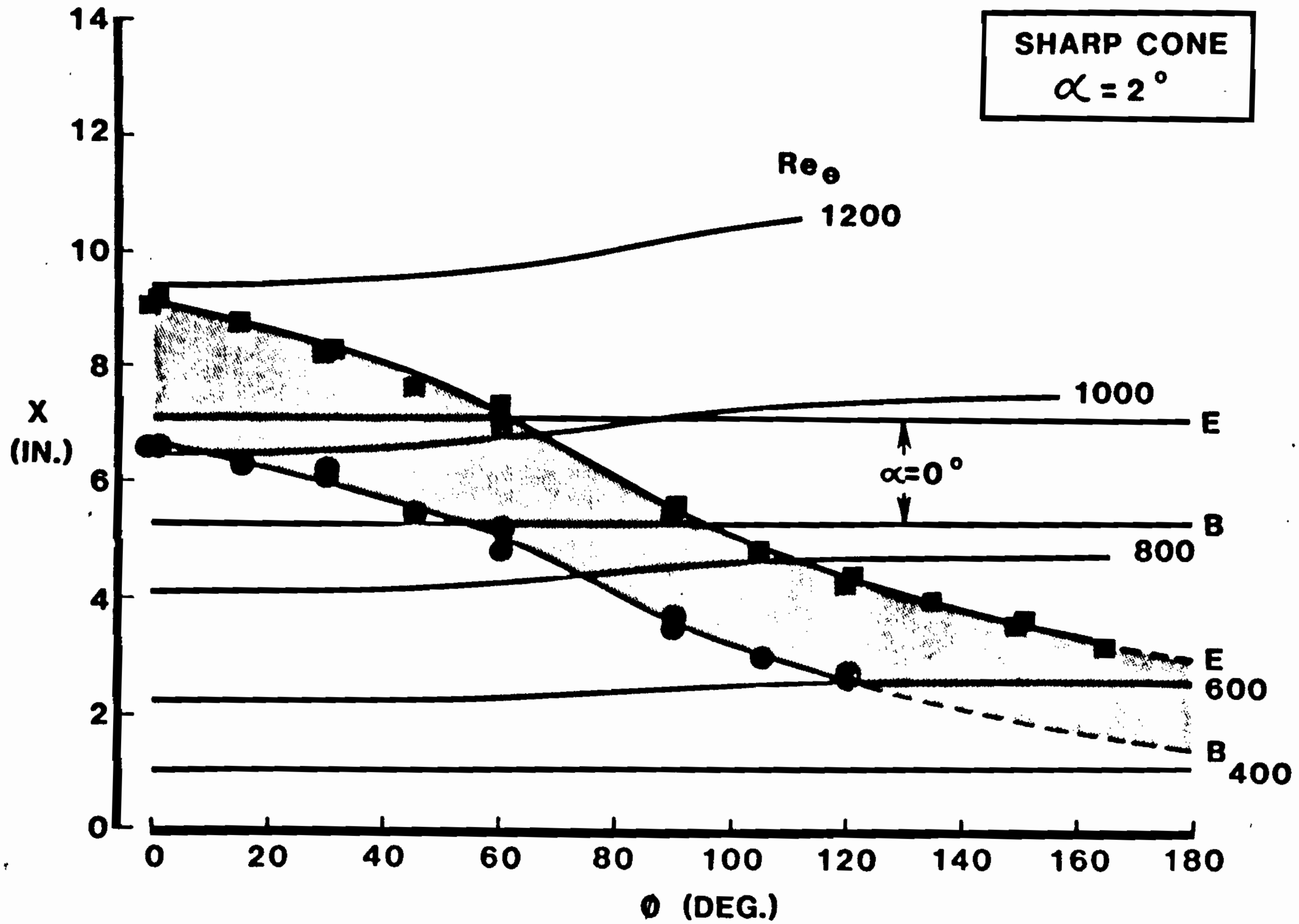

FIG. 10. Transition Pattern on a Sharp Cone at α = 2 Deg.

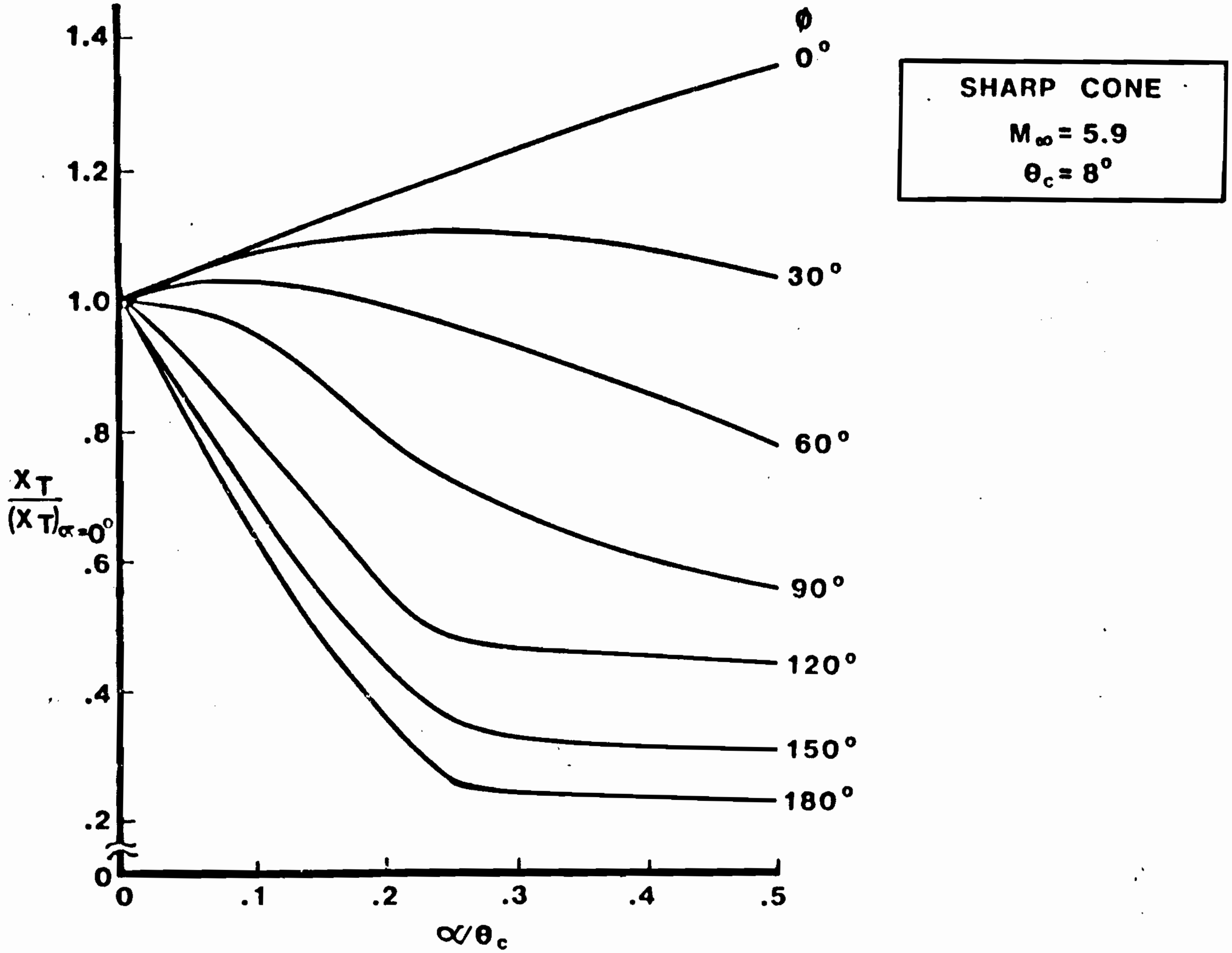

FIG. 11. Transition Asymmetry With Angle of Attack for a Sharp Cone

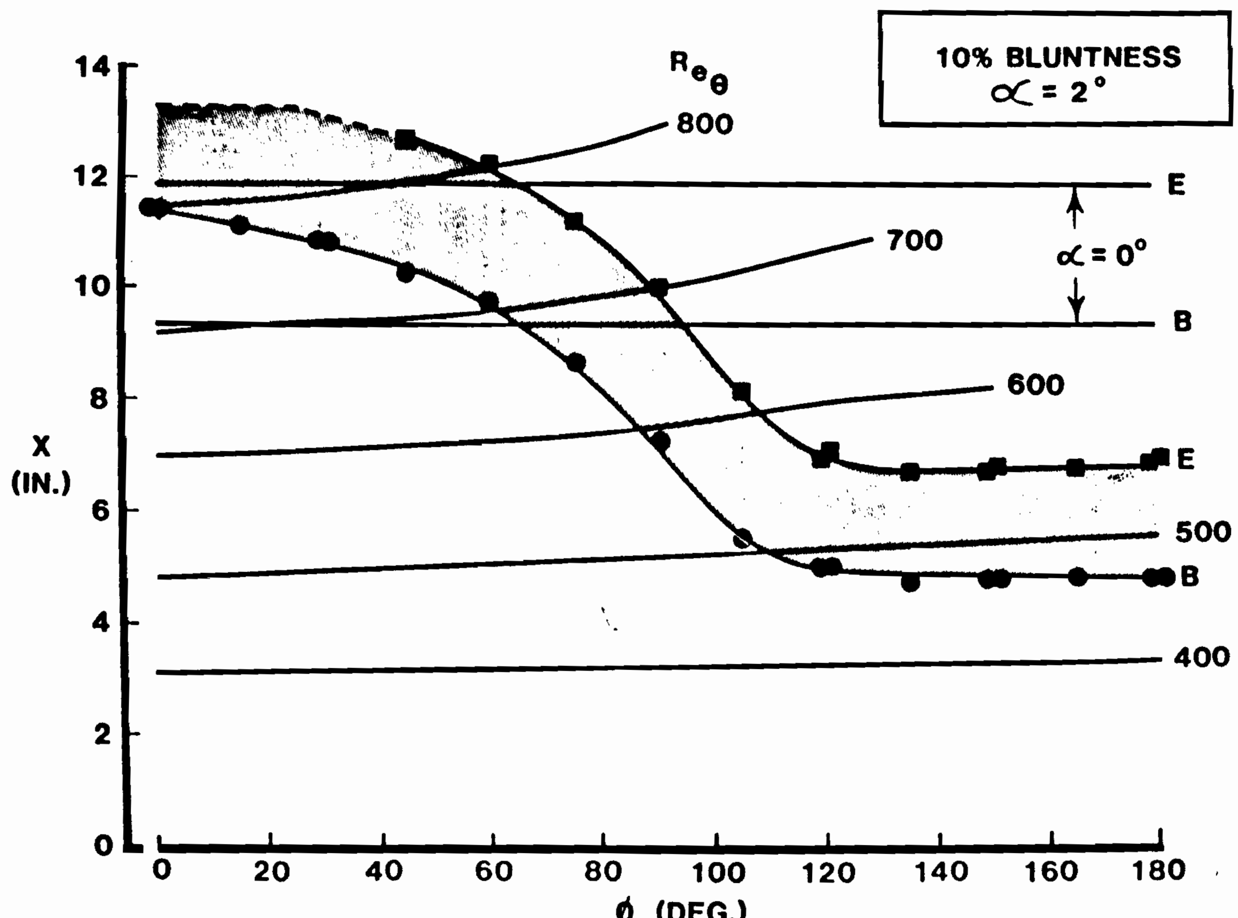

FIG. 12. Transition Pattern on a Blunt Cone at α = 2 Deg.

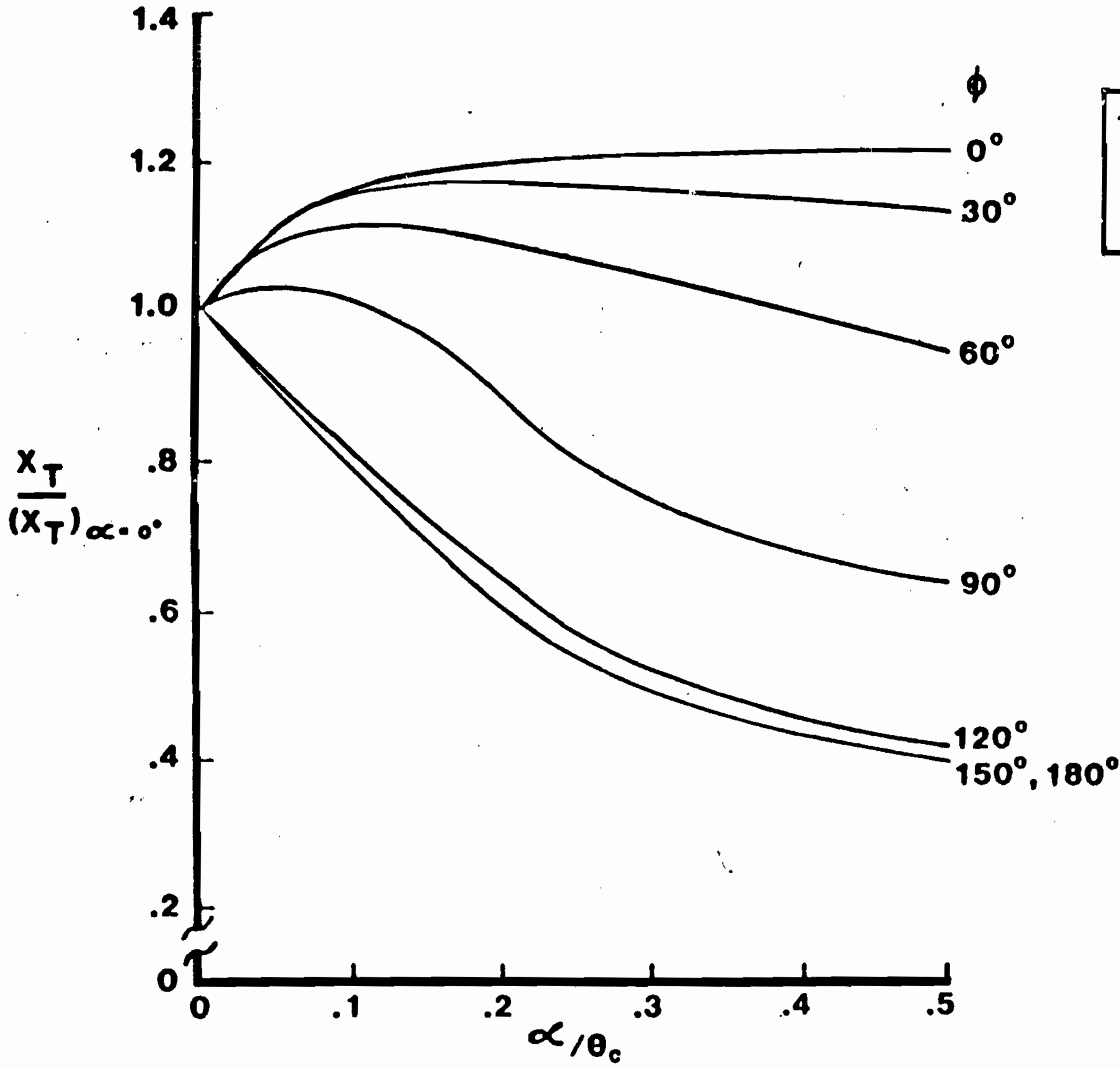

FIG. 13. Transition Asymmetry With Angle of Attack for 10% Nosetip Bluntness

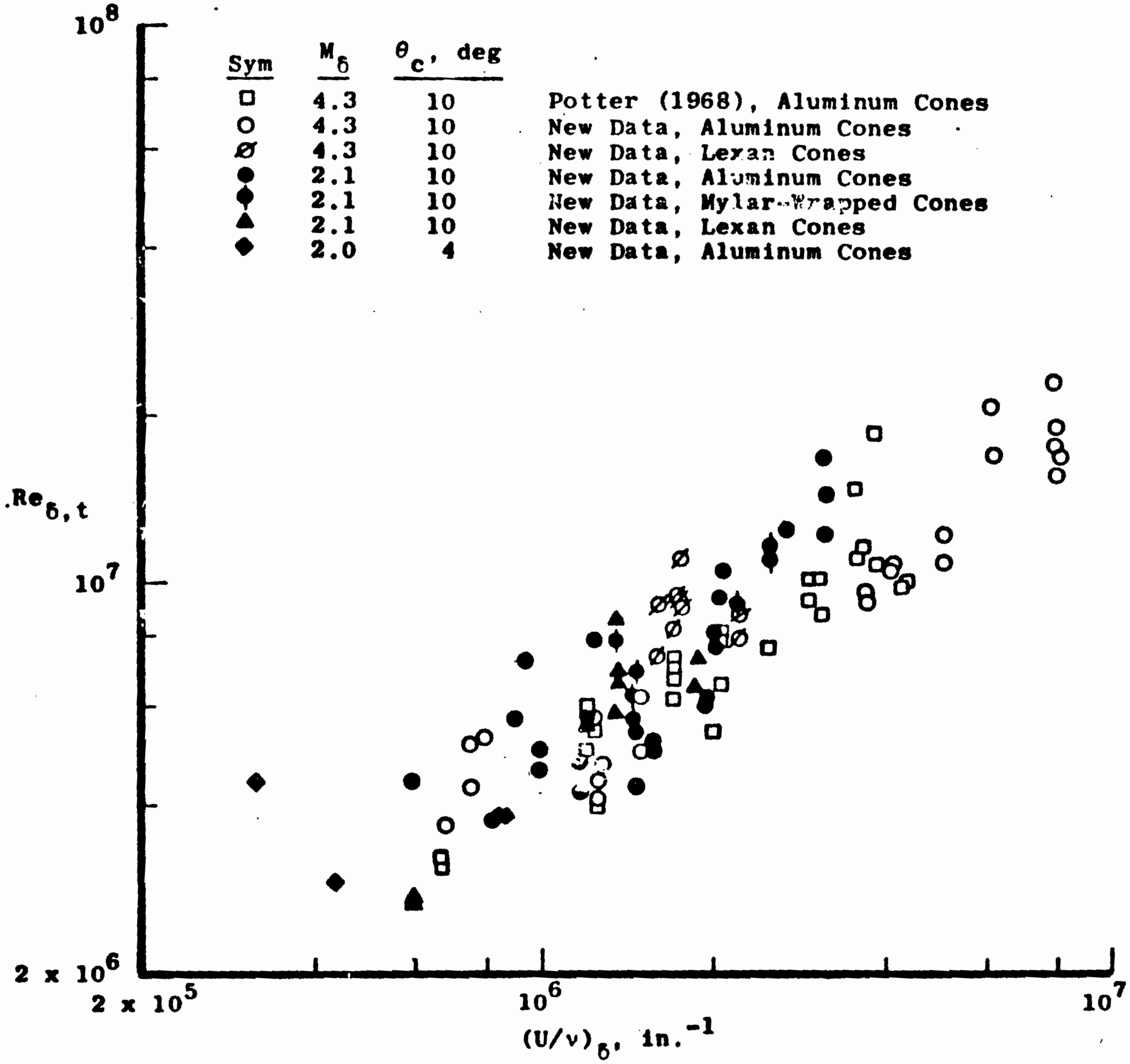

FIG. 14. Unit Reynolds Number Effect in a Ballistic Range

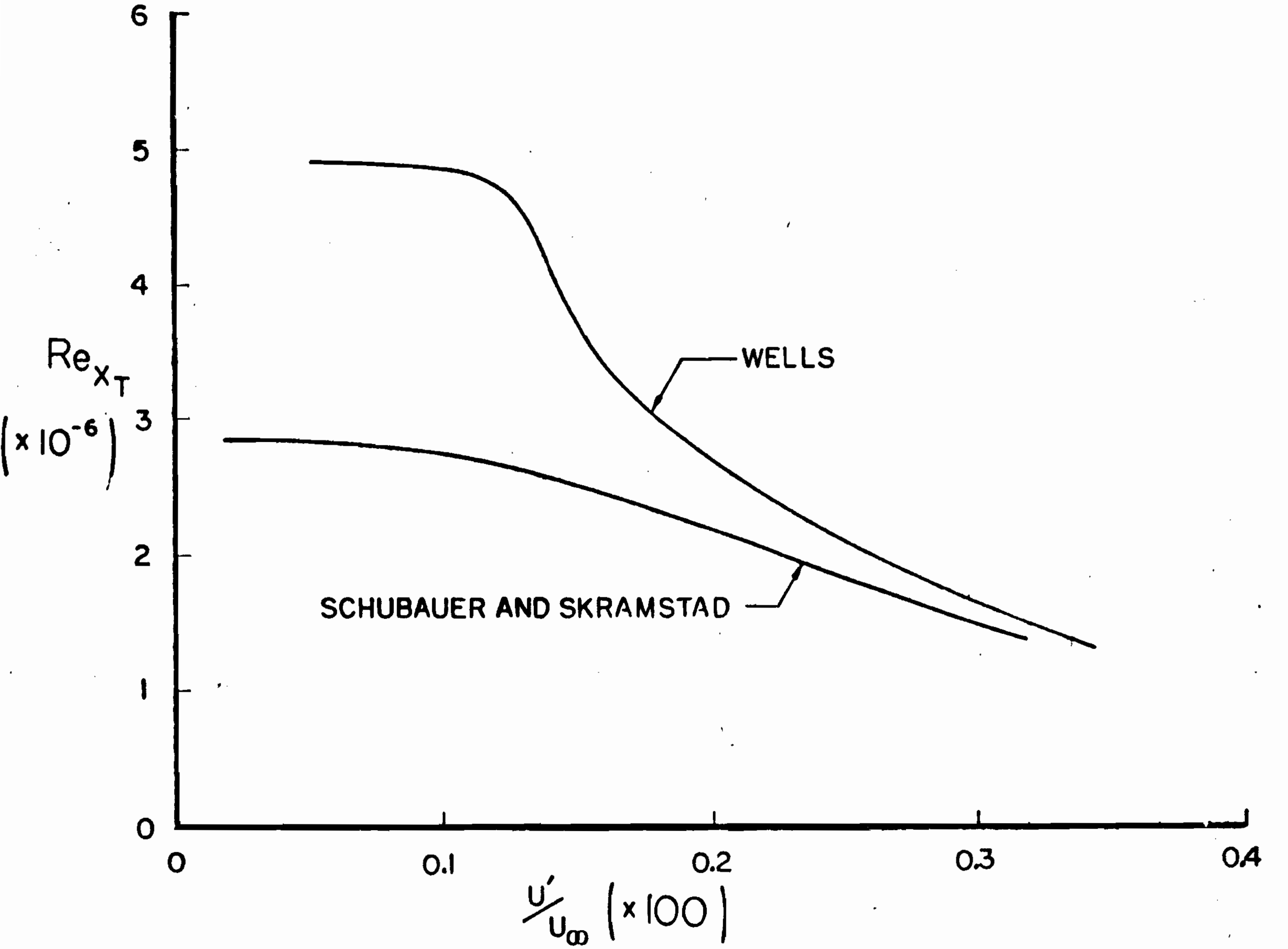

FIG. 15. Effect of Freestream Disturbances on Transition Reynolds Number

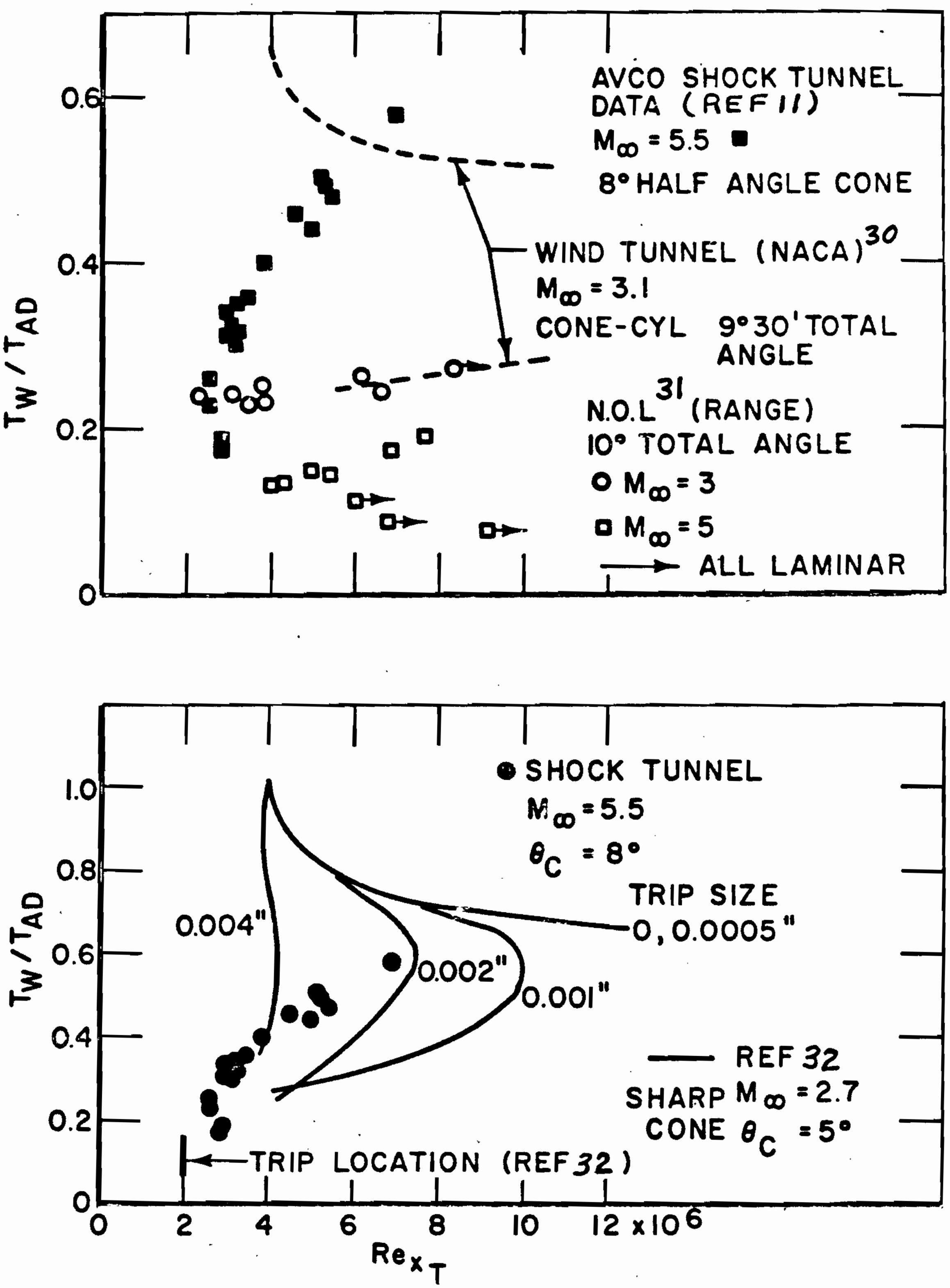

FIG. 16. Effect of Boundary Layer Cooling on Transition

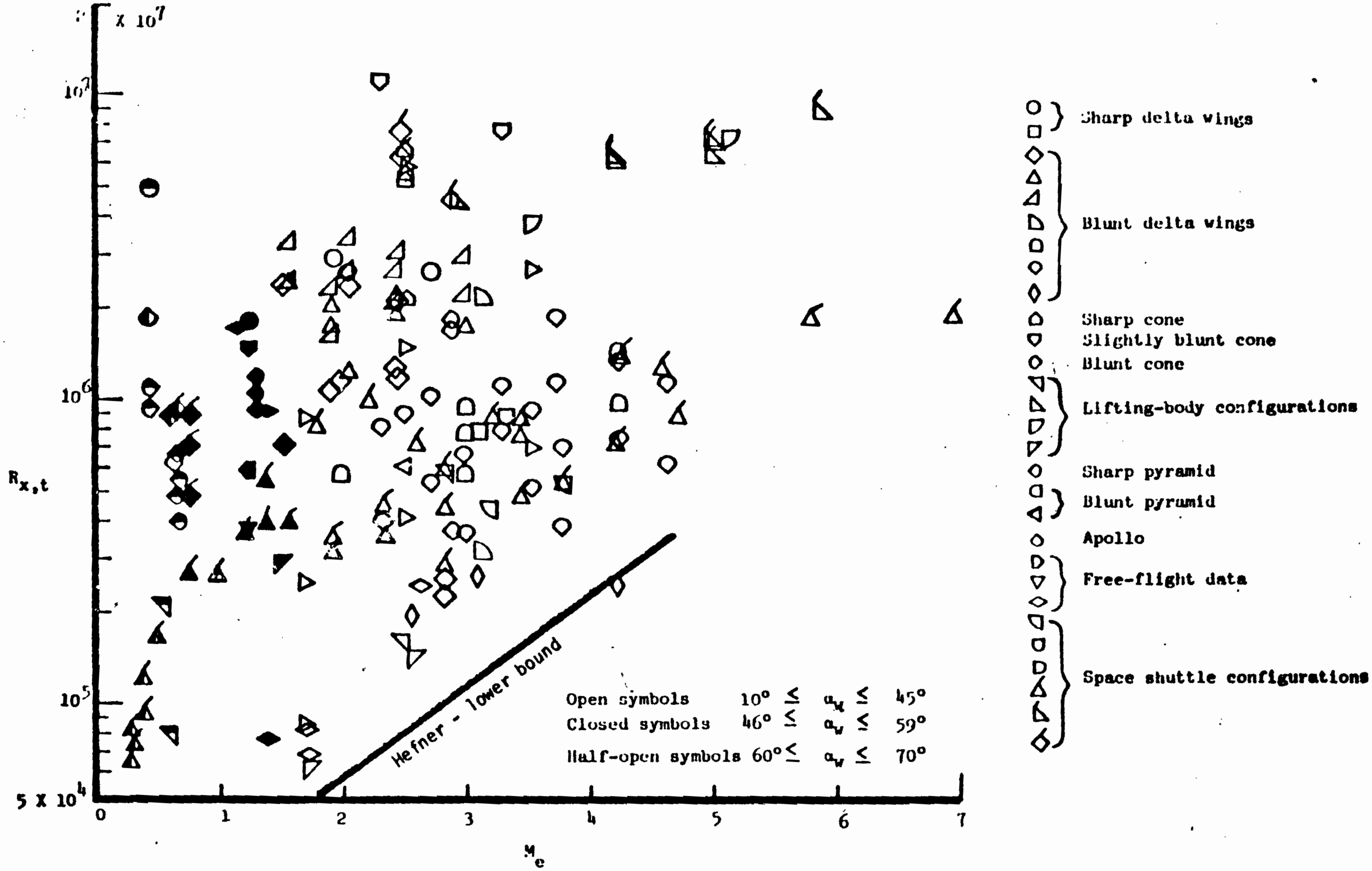

FIG. 17. Transition Reynolds Number as a Function of Local Mach Number

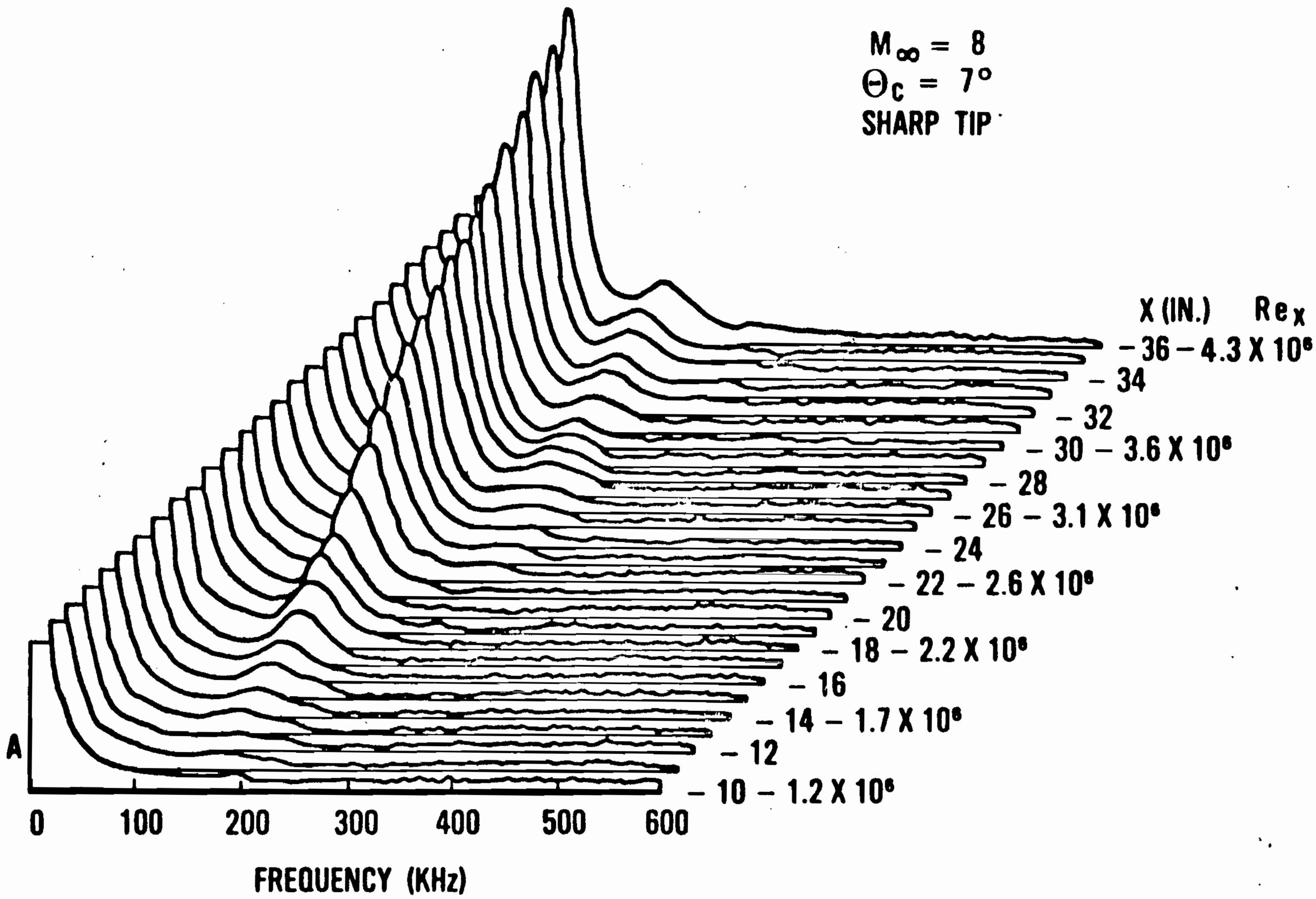

FIG. 18. Boundary Layer Fluctuation Spectra

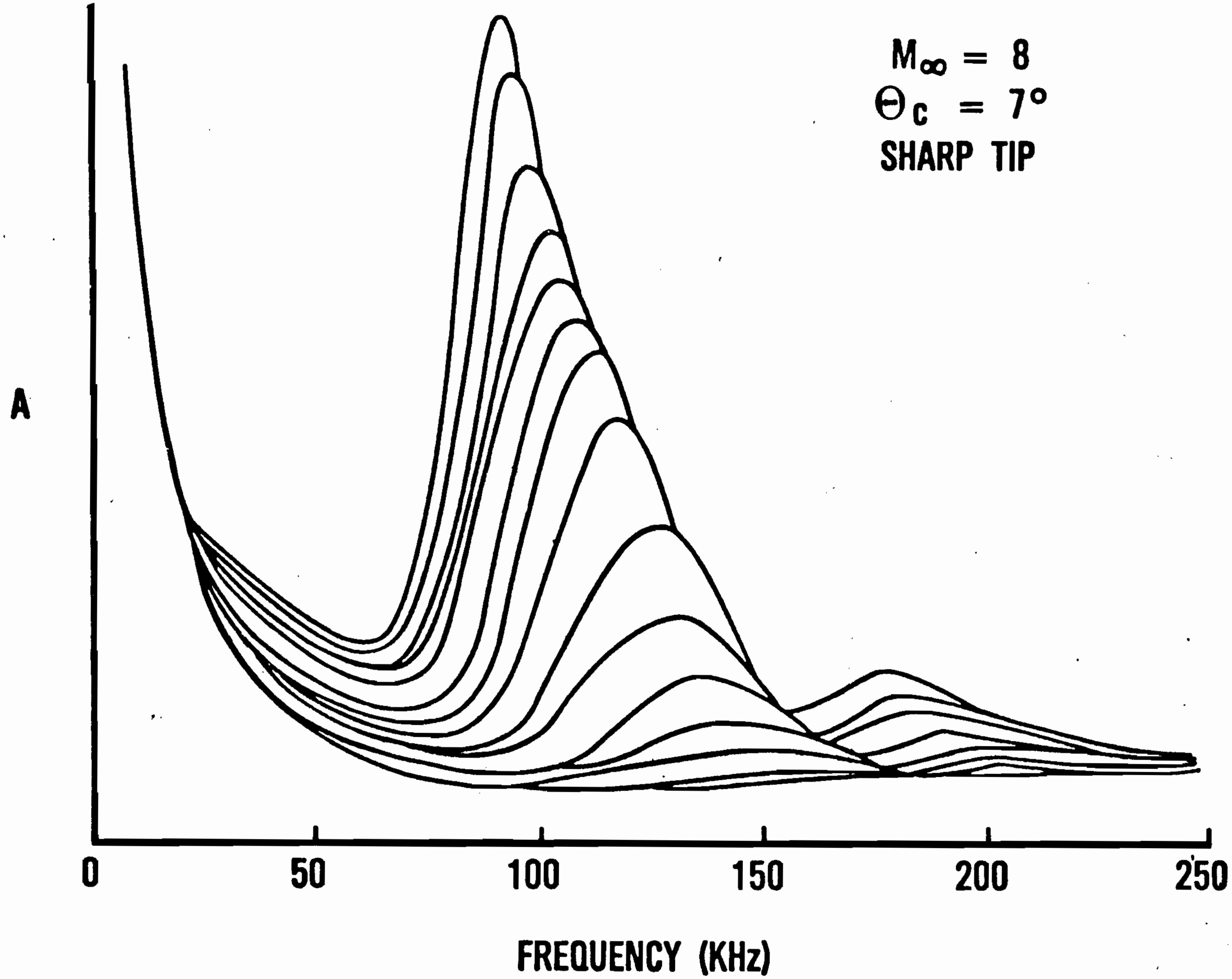

FIG. 19. Fluctuation Spectra Overlayed

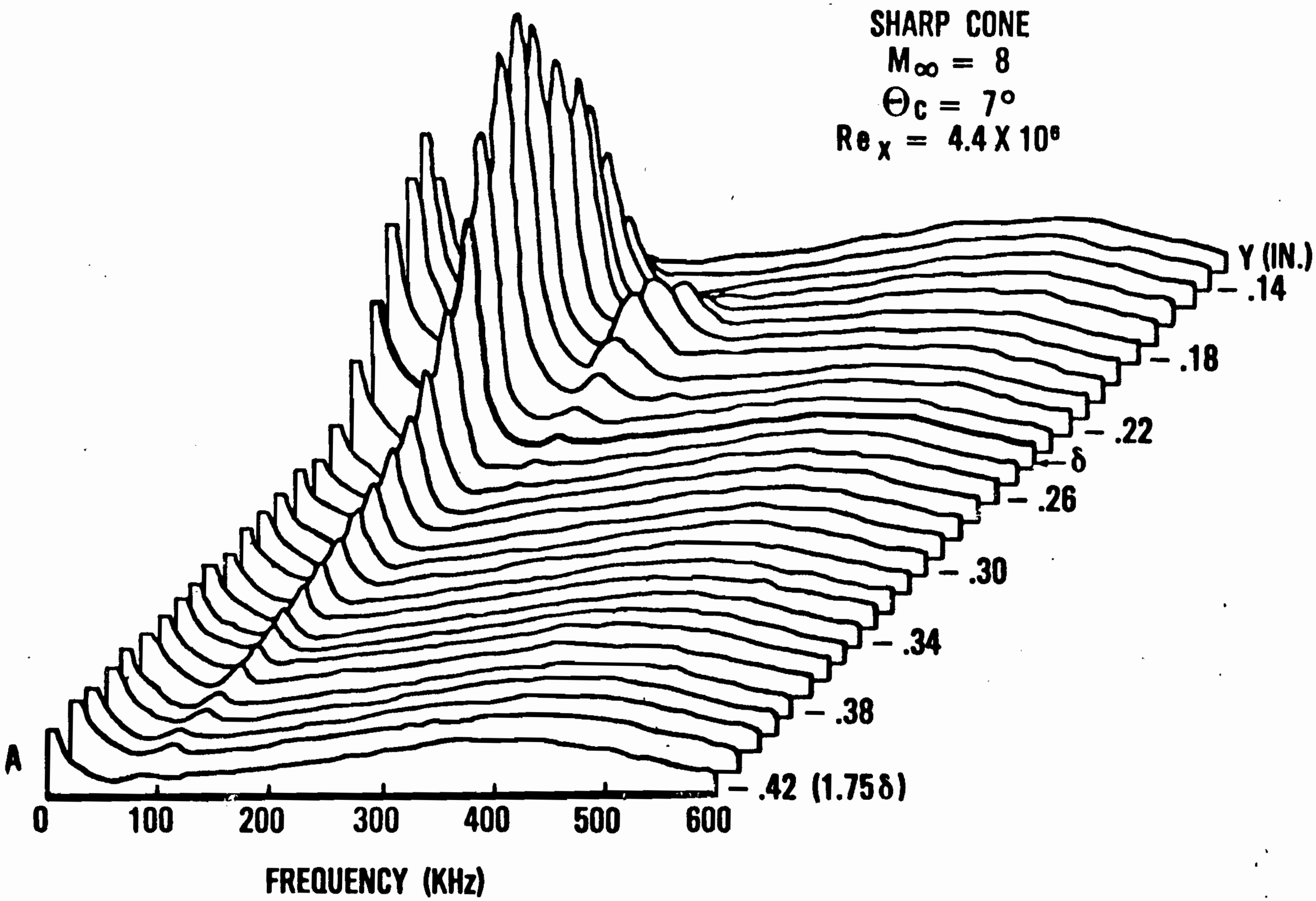

FIG. 20a. Fluctuation Spectra, Normal to the Surface. Outside the Boundary Layer, Looking in

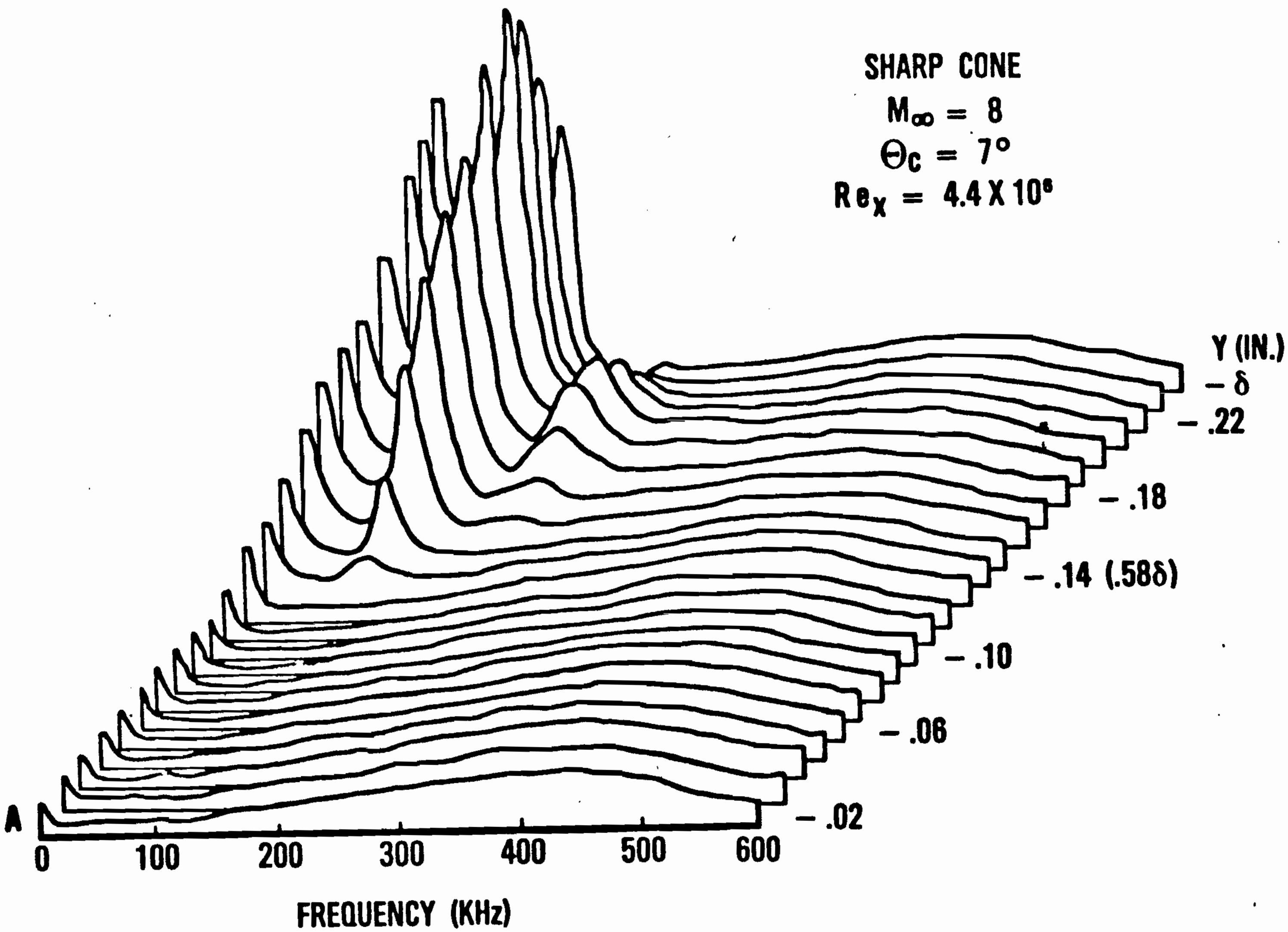

FIG. 20b. Fluctuation Spectra, Normal to the Surface. From the Surface, Looking out

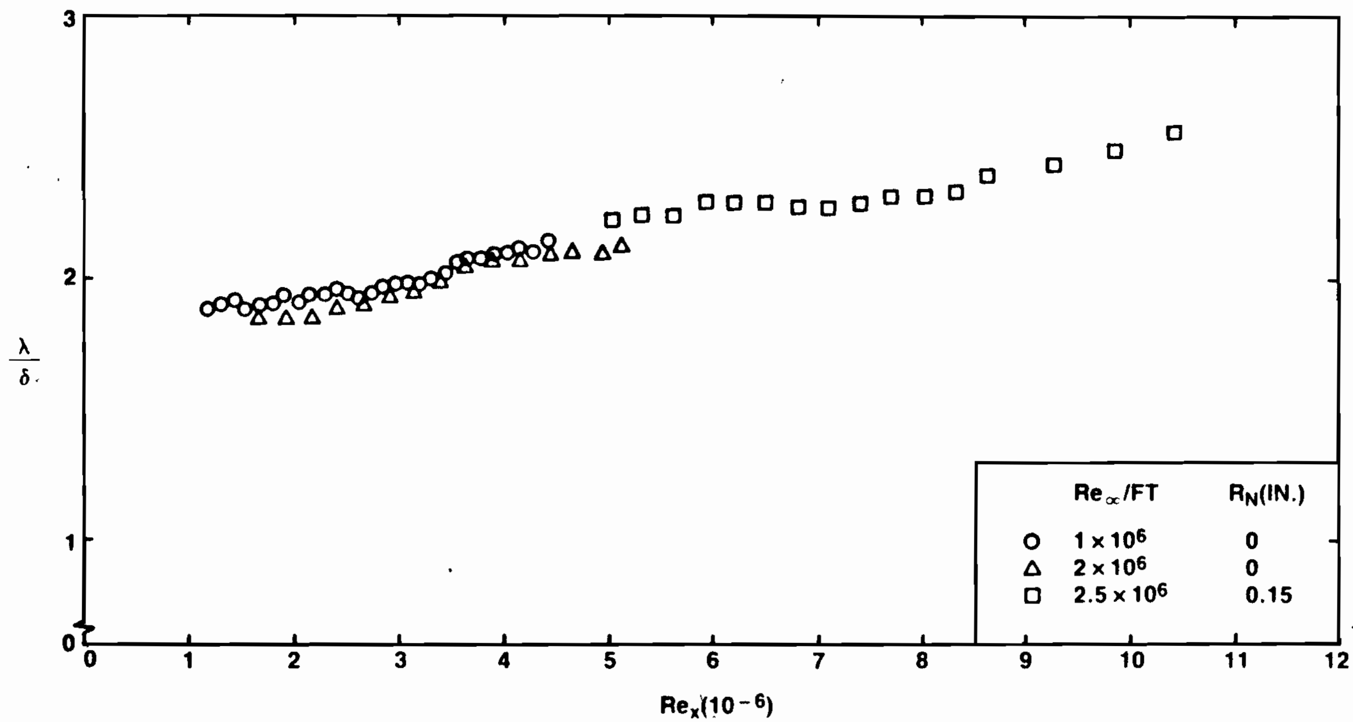

FIG. 21. Wavelengths of the Most Unstable Second Mode Disturbances

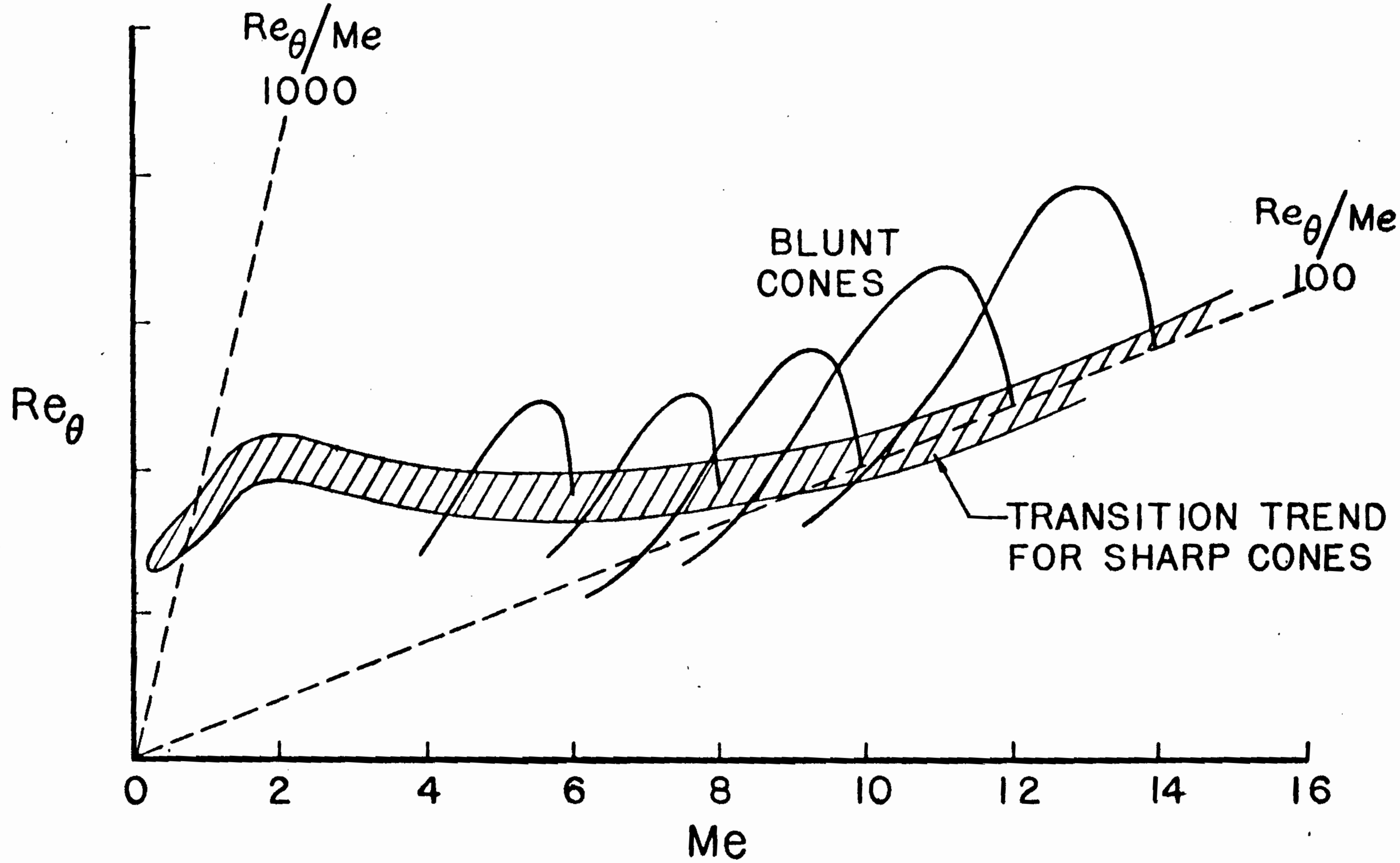

FIG. 22. An Illustration of Re_Θ/Me Variations

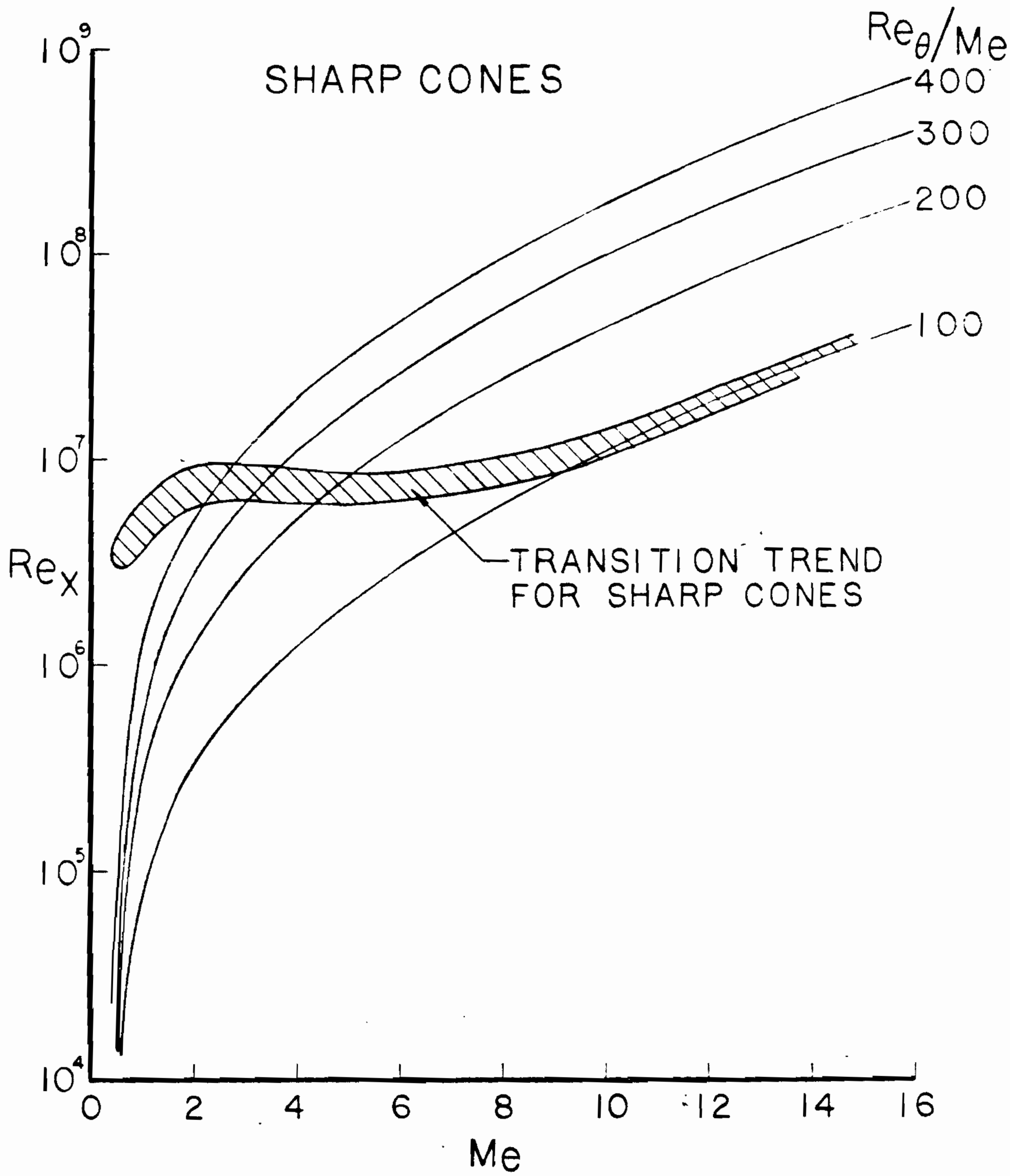

FIG. 23. Re_x Variations as a Function of Re_θ/Me = Constant

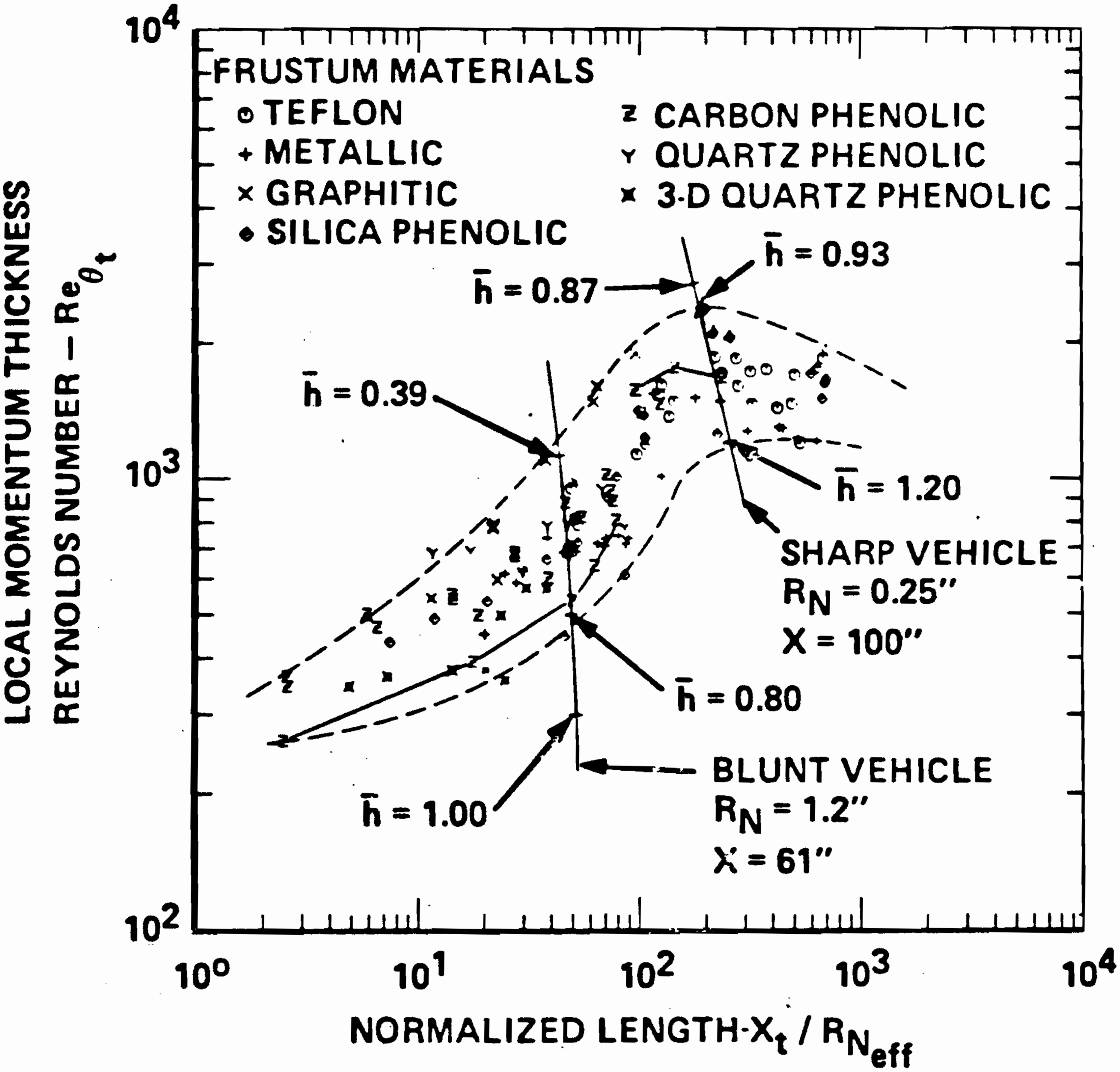

FIG. 24. Re_{Θ_T} vs X/R_N Correlation for Mach 20 Reentry Vehicles

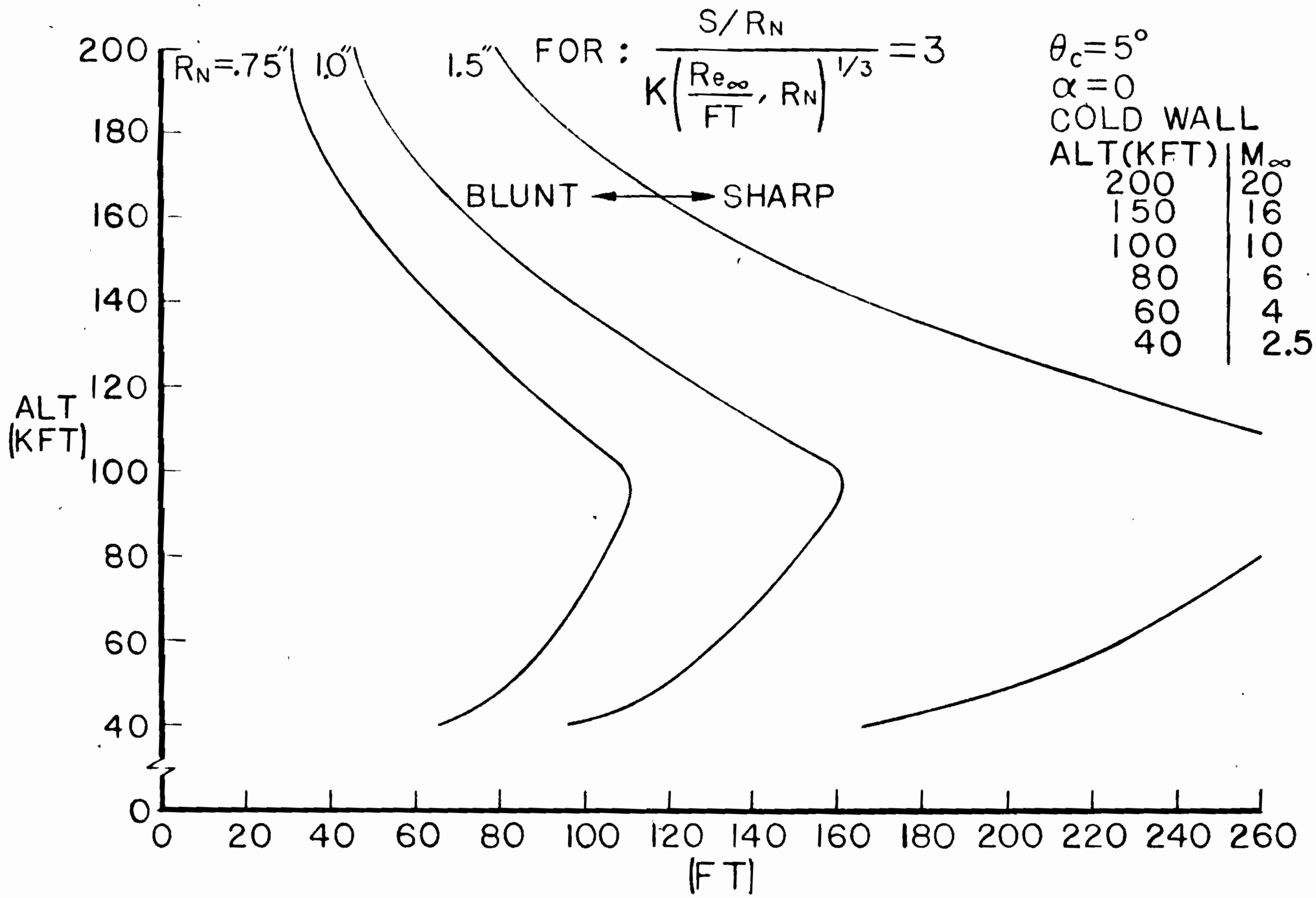

FIG. 25. Entropy Layer Effects on a Slender Cone

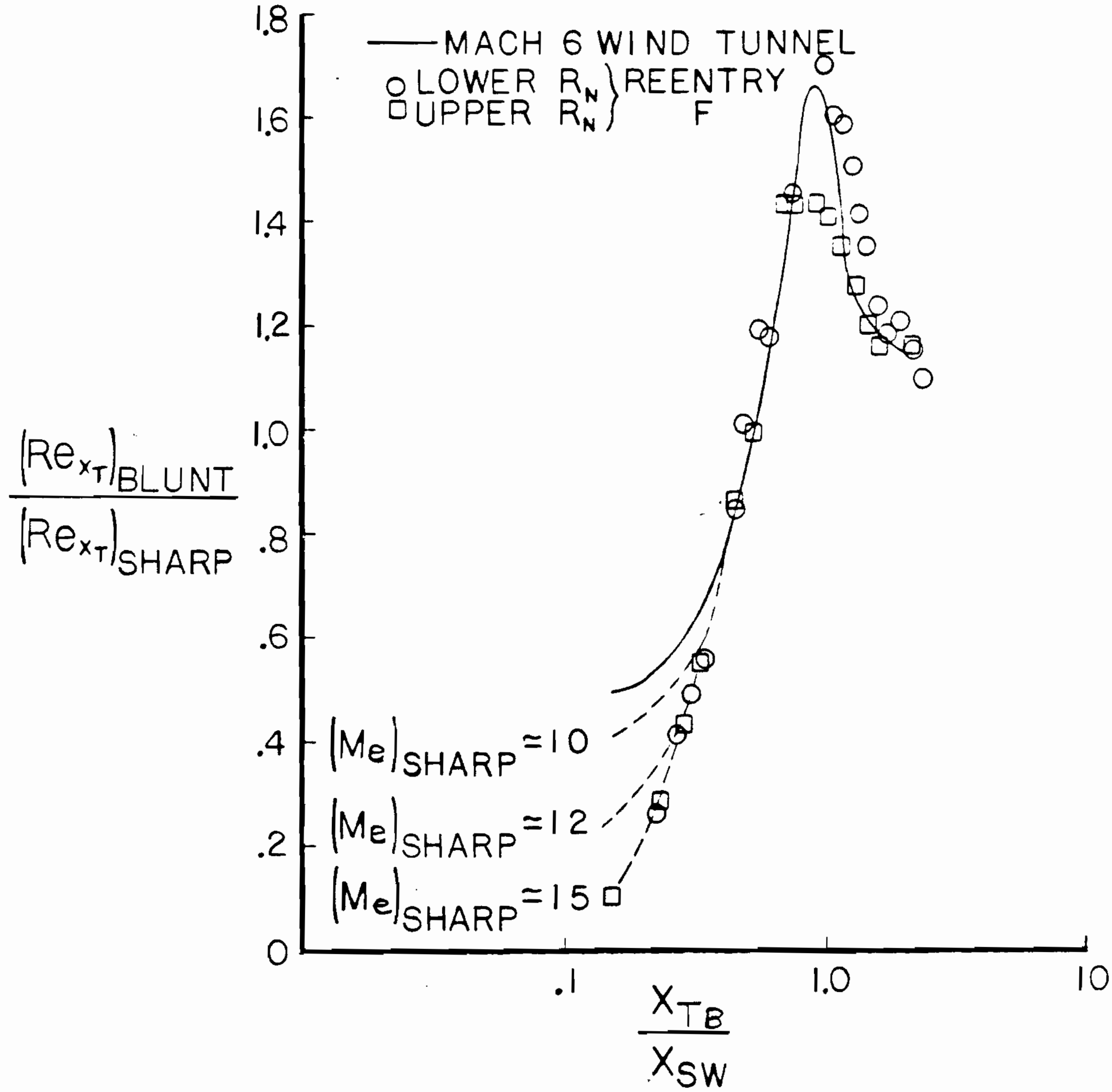

FIG. 26. Transition Reynolds Number Variations Within the Entropy Layer